Formation of Hexagonal Columnar Mesophases by Linear and Branched Oligo- and Polyamides

Markus Seitz,*,† Thomas Plesnivy, Klaus Schimossek, Martin Edelmann, and Helmut Ringsdorf*

Institut für Organische Chemie, Johannes-Gutenberg-Universität, 55099 Mainz, Germany

Hartmut Fischer

Technische Universiteit Eindhoven, Polymer Chemistry & Technology, 5600 MB Eindhoven, The Netherlands

Hiroshi Uyama and Shiro Kobayashi

Department of Materials Chemistry, Graduate School of Engineering, Tohuku University, Sendai 980-77, Japan

Received February 21, 1996; Revised Manuscript Received June 28, 1996[⊗]

ABSTRACT: The formation of columnar mesophases by *N*-acylated azacrown derivatives may be seen as a consequence of their discoid molecular geometry. Viewing these materials as cyclic oligomers, they are just one example of the various molecular architectures that may be realized based on the *N*-acylated ethylenamine fragment. By using linear oligoamides, the hexagonal columnar packing is preserved, the monotropic nature of the mesophase reflecting the higher flexibility of the systems. The corresponding polymers are accessible by polymer analogous acylation of linear poly(ethylenimine), in which a high conversion of the amino groups and a low polydispersity of the final polymers can be achieved. The resulting polyamides form enantiotropic mesophases with a hexagonal columnar structure proven by polarizing microscopy, DSC investigations, and X-ray studies. A helically folded structure of the polymer main chain is proposed whereby this structural motif is probably induced by the packing of the alkyl side chains. Based on side group variations, it was found that the 3,4-bis(alkyloxy)benzoyl side group particularly matches the conformative requirements of the polymer main chain for the formation of a columnar structure. Furthermore, a hexagonal columnar mesophase was observed for a non-symmetrically substituted cinnamoyl side group. Whereas in the case of linear polymers the mesophase is stabilized at higher molecular weights, in the case of branched polyamides the enhanced degree of branching disturbs the chain packing. In the same sense, the introduction of chiral groups both in the polymer main chain and in the side-chain region disturbs the packing into an ordered columnar structure. A monotropic mesophase was found for a regularly branched oligoamide with a presumably discoid molecular structure.

Introduction

The liquid crystalline state combining order and mobility is governed by intermolecular forces between single basic molecular units. These noncovalent interactions are direction dependent for formanisotropic molecules, providing the main driving force for the formation of thermotropic mesomorphic phases.[1,2] However, the relation between the structure of single molecules and the properties of the condensed phase is not always straightforward, since in many cases the same supramolecular structure may be generated from a wide variety of building blocks. In particular, hexagonal columnar mesophases (ϕ_h) are formed by various molecular structures;[3] for example, disk-shaped molecules such as hexaalkoxytriphenylenes exhibit predominantely this type of arrangement (discotic hexagonal mesophase, D_h).[4−7]

The formation of columnar mesophases is not restricted to disk-shaped molecules. Directly comparable are those molecules which due to specific noncovalent interactions form disklike aggregates which then act as mesogenic units.[8,9] Diisobutylsilanediol forms formanisotropic dimers by hydrogen bonding between two premesogens.[10] In a similar fashion, cyclohexanediols[11] as well as numerous nondiscoid carbohydrate derivatives[12−14] build up multimeric aggregates whose columnar packing is supported by the amphiphilic character of the single molecules. In addition, this effect is reflected by the thermotropic hexagonal columnar mesomorphism of several amphiphilic strontium salts.[15] For many rod-, disk-, and bowl-shaped central units, the formation of hexagonal columnar phases is facilitated by the use of the 3,4,5-tris[(*p*-(dodecyloxy)benzyl)oxy]-benzoyl unit (DOBOB), which was first described by Malthête and termed as "columnarogen".[16−18] This and various other taper-shaped units were used by Percec *et al.* to elegantly demonstrate that this sterically induced formation of hexagonal columnar mesophases can be transferred to polymeric compounds. This primarily shape-induced generation of a columnar structure is, to some extent, comparable with the self-organizaiton of the tobacco mosaic virus.[19−27]

In all examples mentioned so far, the columnar phase is formed due to specific interactions between several mesogens or "molecular subunits". In contrast to this, there are numerous polymers lacking any mesogenic unit where one or two polymer chains can form a cylindrical structure. The polymer chain may either be helically folded, as for poly(*n*-alkyl glutamate)s,[28] or take a coiled conformation, as in poly(dialkylsilane)s.[29,30] Additionally, cellulose trialkanoates,[31] poly(phosphazene)s,[32] and several other similar linear polymers radially substituted with side chains belong to this group of polymers with hexagonal columnar meso-

* Authors for correspondence.
† Current address: Department of Chemical Engineering, University of California, Santa Barbara, CA 93106-5080.
⊗ Abstract published in *Advance ACS Abstracts,* September 1, 1996.

S0024-9297(96)00270-7 CCC: $12.00

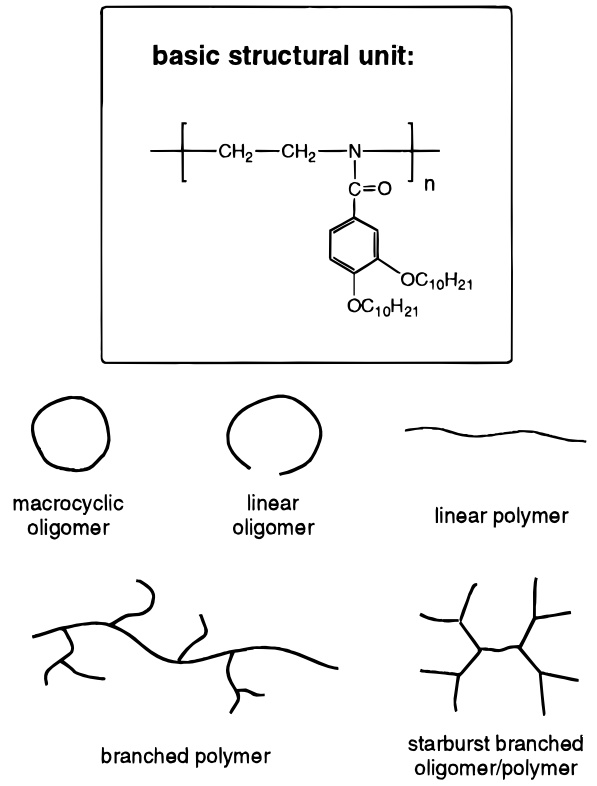

Figure 1. Variation of the molecular architecture of oligo- and polyamides.

phases.[3,33,34]

The formation of hexagonal columnar mesophases by macrocyclic oligoamides was first described by Malthête for a 4-(decyloxy)benzoyl-substituted hexacyclene.[35] The structure was first termed as tubular, but CPK models and force field calculations have since proven that the assumed central "hole" is negligibly small, so this mesophase type cannot be differentiated from the classical discotic mesophase type.[36,37] The mesomorphic character of *N*-acylated azacrown derivatives with benzoyl or cinnamoyl side groups is generally explained by a reduction in the molecular dynamics of the central macrocyclic core.[36,38] However, liquid crystallinity is strongly governed by a balance between the side-chain density and the size of the macrocyclic core, such that smaller azacrowns *N*-substituted with the 3,4-bis(decyloxy)benzoyl group form hexagonal columnar mesophases,[39,40] whereas *N*-acylation with the 4-alkoxybenzoyl or 3,5-bis(decyloxy)benzoyl unit leads to crystalline or glassy materials, respectively.[38] Regarding the generation of a discoid molecular structure, the 3,4-bis(decyloxy)benzoyl side group therefore seems to perfectly match the conformational requirements of azamacrocycles of different ring size.

In general, azacrown derivatives may be regarded as cyclic tetramers of the *N*-acylated ethylenamine fragment, which, as a basic structural unit, can build up oligomeric as well as polymeric compounds of different molecular architecture (Figure 1).

Recently, we have shown that even a linear polyamide ($n = 22$) based on this structural unit exhibits a hexagonal columnar mesophase.[40] The synthesis of the same polymer with fewer repeat units,[41] which shows a lower clearing point as well as the monotropic nature of defined oligomers ($n = 3-5$),[40,42,43] reflecting their higher conformational flexibility, reveals the obvious influence of the polymer main chain in these systems. In this paper, we present a systematic study of the influence of the degree of polymerization and the effects of side-chain variations as well as of the main-chain topology on the formation of a hexagonal columnar mesophase in noncyclic polyamides. Furthermore, the introduction of a chiral group in the side chains and in the polymer main chain of the linear polymers will be discussed.

Experimental Section

Materials. Linear poly(ethylenimine)s of different degrees of polymerization were synthesized by zwitterionic ($n = 22$)[44] or cationic ring-opening polymerization ($n = 10, 51, 186$).[45,46] Linear oligomers ($n = 4, 5$) 1,4,7,10-tetraazadecane and 1,4,7,10,13-pentaazatridecane were purchased as hydrochlorides (Aldrich). For deprotonation, an appropriate excess of DMAP was used during the acylation reaction. Branched poly(ethylenimine) of high molecular weight ($n = 230$) was obtained as a commercial product from Polyscience. The branched oligomeric samples as well as the dendrimeric oligomer were provided by the BASF AG (Ludwigshafen, Germany).

4-(Decyloxy)benzoyl chloride, 3,4-bis(decyloxy)benzoyl chloride, 3,4,5-tris(decyloxy)benzoyl chloride, and 4-(dodecyloxy)-cinnamoyl chloride as well as 4-(dodecyloxy)-3-methoxycinnamoyl chloride were synthesized according to known literature procedures from the appropriate acids with oxalyl chloride in toluene.[38] 4-(Dodecyloxy)-3-methoxycinnamic acid was prepared in two steps from 3-methoxy-4-hydroxybenzaldehyde (vanillin) by alkylation with 1-bromododecane and successive Knoevenagel condensation with malonic acid.[47] Synthesis of the chiral 4-(heptyloxy)-3-[(*S*)-(1-methylheptyl)oxy]benzoyl chloride was performed in three steps, starting from ethyl 3,4-dihydroxybenzoate (Aldrich).

Ethyl 4-(Heptyloxy)-3-hydroxybenzoate. Ethyl 3,4-dihydroxybenzoate (7 g, 38.4 mmol) was stirred under reflux with 1-bromoheptane (6.88 g, 38.4 mmol), dry K_2CO_3 (5.84 g, 42.2 mmol), and traces of potassium iodide in 200 mL of dry acetone under an argon atmosphere for 1 day. The hot reaction mixture was filtered, the residue extracted with 300 mL of warm acetone, and the solvent removed from the combined solutions. Flash chromatography (petroleum ether/ethyl acetate 10:1) yielded a mixture of the two constitutional isomers, which can be separated by twofold recrystallization from hexane. Whereas ethyl 4-(heptyloxy)-3-hydroxybenzoate was only fairly soluble and crystallized from hexane at room temperature as white needles, the mother liquor contained predominantly ethyl 3-(heptyloxy)-4-hydroxybenzoate. Yield: 3.9 g (36%) of ethyl 4-(heptyloxy)-3-hydroxybenzoate (side product, 1.1 g (10%) of ethyl 3-(heptyloxy)-4-hydroxybenzoate); mp 80 °C; $R_f = 0.40$ (petroleum ether/ethyl acetate 5:1). ^{1}H NMR, mass spectrum, and elemental analysis data were in accordance with the proposed structure. The structure of the compound with regard to alkylation in the 4-position was proven by X-ray structural analysis.

Ethyl 4-(Heptyloxy)-3-[(*S*)-(1-methylheptyl)oxy]benzoate. To a solution of ethyl 4-(heptyloxy)-3-hydroxybenzoate (3.7 g, 13.2 mmol), (*R*)-2-octanol (2.1 g, 15.9 mmol), and triphenylphosphine (4.2 g, 15.9 mmol) in 35 mL of dry THF, diethyl azodicarboxylate (2.8 g, 15.9 mmol) dissolved in 10 mL of dry THF was added slowly at room temperature. After the mixture was stirred under an argon atmosphere at room temperature for 2 h, the reaction was stopped by the addition of 4 mL of water. The solvent was evaporated and the product isolated by flash chromatography (petroleum ether/ethyl acetate 20:1, $R_f = 0.35$) to yield 3.84 g (74%) of a white solid, mp 28 °C. The ^{1}H NMR and elemental analysis data were in accordance with the proposed structure.

4-(Heptyloxy)-3-[(*S*)-1-(methylheptyl)oxy]benzoic Acid. Ethyl 4-(heptyloxy)-3-[(*S*)-(1-methylheptyl)oxy]benzoate (3.34 g, 8.51 mmol) and potassium hydroxide (0.57 g, 10.2 mmol) were refluxed in a mixture of 80% (v/v) ethanol in water (60 mL) for 8 h. After that, 10 mL of water was added, and the reaction mixture was acidified to pH 1 with concentrated

hydrochloric acid. The precipitate was filtered, washed with cold water, and recrystallized from acetic acid. After the crystals were dried in vacuo at 60 °C for several hours, 3.0 g (98%) of the acid was obtained as a white, crystalline powder: mp 84 °C; R_f = 0.40 (petroleum ether/ethyl acetate 1:1); ^{1}H NMR ($CDCl_3$, 200 MHz) δ 0.87 (m, 6H, CH_3(CH$_2$)$_4$), 1.15−1.7 (m, 20H, CH$_3$(CH_2)$_4$, CH$_2$CH(CH_3)OAr, and CHH-CH(CH$_3$)OAr), 1.81 (m, 3H, CH_2CH$_2$OAr and CHH-CH(CH$_3$)OAr), 4.03 (t, 2H, CH_2OAr), 4.34 (m, 1H, CH$_3$CH(CH$_3$)OAr), 6.88 (d, 1H, Ar H-5), 7.61 (d, 1 H, Ar H-2), 7.72 (dd, 1H, Ar H-6); mass spectrum, *m/e* 364.8. Anal. Calcd for $C_{22}H_{36}O_4$ (M_r = 365.56): C, 72.29; H, 9.92. Found: C, 71.15; H, 9.78.

The *N*-acylation of polymeric as well as oligomeric amines with the substituted benzoyl chlorides was performed in absolute DMF with DMAP as a base according to the following general procedures.

1,4,7,10-Tetrakis[3,4-bis(decyloxy)benzoyl]-1,4,7,10-tetraazadecane (N(4)-3,4). A mixture of 1,4,7,10-tetraazadecane tetrahydrochloride (480 mg, 1.64 mmol), 3,4-bis(decyloxy)-benzoyl chloride (3.0 g, 6.62 mmol), and DMAP (1.61 g, 13.2 mmol) was stirred in 40 mL of dry dichloromethane under an argon atmosphere for 1 day. The cooled reaction mixture was poured into 150 mL of 2 N HCl, and the organic layer was separated and washed with water two times. The solution was dried with natrium sulfate and distilled to complete dryness and the resulting crude product was heated with acetone for 5 min. The solid residue was collected by filtration of the hot suspension and purified by flash chromatography (dichloromethane/methanol 60:1), dissolved in dichloromethane, and precipitated in cold acetone to yield 1.30 g (44%) of a white solid: mp 99 °C; R_f = 0.35 (chloroform/methanol 40:1); ^{1}H NMR ($CDCl_3$, 200 MHz) δ 0.85 (t, 24H, CH_3(CH$_2$)$_9$O), 1.1−1.5 (m, 112H, CH$_3$(CH_2)$_7$CH$_2$CH$_2$O), 1.63 (m, 16H, CH$_3$(CH$_2$)$_7$CH_2-CH$_2$O), 3.3−3.8 (m, 12H, CH_2N), 3.8−4.0 (m, 16H, CH$_3$-(CH$_2$)$_8$CH_2O),6.5−7.0 (m, 8H, Ar H-2,5,6 of tertiary amides and Ar H-5 of secondary amides), 7.2−7.6 (m, 6H, Ar H-2,6 of secondary amides and NHCO); mass spectrum, *m/e* 1813.7. Anal. Calcd for $C_{114}H_{194}N_4O_{12}$ (M_r = 1812.94): C, 75.53; H, 10.79; N, 3.09. Found: C, 75.27; H, 10.79; N, 3.19.

1,4,7,10,13-Pentakis[3,4-bis(decyloxy)benzoyl]-1,4,7,10,13-pentaazatridecane (N(5)-3,4): mp 117 °C; R_f = 0.60 (chloroform/methanol 25:1). ^{1}H NMR, mass spectrum, and elemental analysis data were in accordance with the proposed structure.

Poly(*N*-[3,4-bis(decyloxy)benzoyl]ethylenimine) (LPEI-(22)-3,4). 3,4-Bis(decyloxy)benzoyl chloride (4.52 g, 10 mmol), linear poly(ethylenimine) (0.4 g, 9.3 mmol), and (*N*,*N*-dimethylamino)pyridine (DMAP) (1.3 g, 11 mmol) were stirred for 3 days at 70 °C in 150 mL of absolute *N*,*N*-dimethylformamide (DMF) in an argon atmosphere. The white precipitate was separated and dried for 2 days under high vacuum to remove the solvent. The crude product was suspended in dichloromethane and successively washed with 1 N aqueous NaOH twice and three times with water. After drying with anhydrous sodium sulfate, the solution was concentrated and filtered through a micrometer-size filter, and the polymer was precipitated in cold acetone. This procedure was repeated (purity of the product checked by TLC from dichloromethane/methanol mixtures) and the polymer finally recrystallized from acetone, yielding 1.4 g of a white powder. According to elemental analysis and ^{1}H NMR spectroscopy, the polymer analogous acylation was almost quantitative (>95%): ^{1}H NMR (200 MHz, $CDCl_3$) δ 0.85 (t, 6H, CH_3(CH$_2$)$_9$O), 1.1−1.4 and 1.5−1.9 (br, 32H, CH$_3$(CH_2)$_8$CH$_2$O), 3.3−3.6 (br, 4H, CH_2-NCH_2), 3.8−4.0 (br, 4H, CH$_3$(CH$_2$)$_8$CH_2O), 6.6−6.8 (br, 3H, Ar H-2,5,6); Anal. Calcd for $(C_{29}H_{49}NO_3)_n$ (corresponding to a 100% substitution; $M_{rep.unit}$ = 459.72): C, 75.77; H, 10.74; N, 3.05 (C/N = 24.84). Found: C, 75.40; H, 10.63; N, 2.94 (C/N = 25.64). Degree of substitution calculated from C/N ratio, >95%. GPC ($CHCl_3$; polystyrene standard): M_n = 10 500 (calcd for P_n = 22, M_n = 10 114), M_w = 12 000.

LPEI(11)-3,4. Anal. Found: C, 75.83; H, 10.59; N, 2.72 (C/N = 27.88). Degree of substitution calculated from C/N ratio, >95%. GPC ($CHCl_3$; polystyrene standard): M_n = 5400 (calcd for P_n = 11, M_n = 5057), M_w = 5900.

LPEI(51)-3,4. Anal. Found: C, 75.23; H, 10.62; N, 2.98 (C/N = 25.25). Degree of substitution calculated from C/N ratio >95%. GPC ($CHCl_3$; polystyrene standard): M_n = 16 200 (calcd for P_n = 51, M_n = 23 446), M_w = 19 200.

LPEI(186)-3,4. Anal. Found: C, 74.61; H, 11.04; N, 3.06 (C/N = 24.38). Degree of substitution calculated from C/N ratio, >95%. GPC ($CHCl_3$; polystyrene standard): M_n = 24 500 (calcd for P_n = 186, M_n = 85 508), M_w = 47 100.

Note that the determination of the molecular weight relative to a polystyrene standard leads to a relatively high deviation compared to the expected, calculated value for the last polymer, **LPEI(186)-3,4**. Nevertheless, as in the case of the lower molecular weight samples, the degree of substitution as determined by ^{1}H NMR and elemental analysis is above 95%, and a chain degradation during the acylation reaction can be excluded. However, as we cannot give absolute molecular weight numbers at this stage, it should be kept in mind that the number *n* given in parentheses corresponds to the degree of polymerization of the starting material, the unsubstituted linear poly(ethylenimine).

Characterization of the Obtained *N*-Acylated Polymers. The degree of substitution and the molecular weights of the other polymers were calculated from elemental analysis and GPC data as given below. Their ^{1}H NMR data were in agreement with the proposed structures. These data are included in the supporting information.

Poly(*N*-[4-(decyloxy)benzoyl]ethylenimine) (LPEI(22)-4). Anal. Calcd for $(C_{19}H_{29}NO_2)_n$ (corresponding to a 100% substitution; $M_{rep.unit}$ = 303.45): C, 75.21; H, 9.63; N, 4.62 (C/N = 16.28). Found: C, 73.15; H, 9.86; N, 4.94 (C/N = 14.81). Degree of substitution calculated from C/N ratio, ∼90%. GPC ($CHCl_3$; polystyrene standard): M_n = 4400 (calcd for P_n = 22, 100% substitution, M_n = 6676), M_w = 5600.

Poly(*N*-[3,4,5-tris(decyloxy)benzoyl]ethylenimine) (LPEI(22)-3,4,5). Anal. Calcd for $(C_{39}H_{69}NO_4)_n$ (corresponding to a 100% substitution; $M_{rep.unit}$ = 615.99): C, 76.05; H, 11.29; N, 2.27 (C/N = 33.50). Found: C, 75.78; H, 10.85; N, 2.75 (C/N = 27.56). Degree of substitution calculated from C/N ratio, ∼80%. GPC ($CHCl_3$; polystyrene standard): M_n = 8100 (calcd for P_n = 22, 100% substitution, M_n = 13 376), M_w = 9000.

Poly(*N*-[3,5-bis(decyloxy)benzoyl]ethylenimine) (LPEI-(22)-3,5). Anal. Calcd for $(C_{29}H_{49}NO_3)_n$ (corresponding to a 100% substitution; $M_{rep.unit}$ = 459.72): C, 75.77; H, 10.74; N, 3.05 (C/N = 24.84). Found: C, 73.52; H, 10.72; N, 3.06 (C/N = 24.02) Degree of substitution calculated from C/N ratio, ∼95%. GPC (THF; polystyrene standard): M_n = 7600 (calcd for P_n = 22, 100% substitution, M_n = 10 114), M_w = 13 000.

Poly(*N*-[4-(dodecyloxy)cinnamoyl]ethylenimine) (LPEI-(22)-Cinn12,H). Anal. Calcd for $(C_{23}H_{35}NO_2)_n$ (corresponding to a 100% substitution; $M_{rep.unit}$ = 357.54): C, 77.27; H, 9.87; N, 3.92 (C/N = 19.71). Found: C, 76.07; H, 9.67; N, 3.43 (C/N = 22.18). Degree of substitution calculated from C/N ratio, >95%. GPC ($CHCl_3$; polystyrene standard): M_n = 8300 (calcd for P_n = 22, 100% substitution, M_n = 7866), M_w = 12 800.

Poly(*N*-[4-(dodecyloxy)-3-methoxycinnamoyl]ethylenimine) (LPEI(22)-Cinn12,OMe). Anal. Calcd for $(C_{24}H_{37}NO_3)_n$ (corresponding to a 100% substitution; $M_{rep.unit}$ = 387.57): C, 74.38; H, 9.62; N, 3.61 (C/N = 20.60). Found: C, 72.90; H, 10.85; N, 4.03 (C/N = 18.09). Degree of substitution calculated from C/N ratio >95%. GPC ($CHCl_3$; polystyrene standard): M_n = 6000 (calcd for P_n = 22, 100% substitution, M_n = 8527), M_w = 8100.

Poly(*N*-[3,4-bis(heptyloxy)benzoyl]ethylenimine) (LPEI(22)-3,4/7). Anal. Calcd for $(C_{23}H_{37}NO_3)_n$ (corresponding to a 100% substitution; $M_{rep.unit}$ = 375.56): C, 73.56; H, 9.93; N, 3.73 (C/N = 19.72). Found: C, 71.95; H, 10.55; N, 3.63 (C/N = 19.82). Degree of substitution calculated from C/N ratio, >95%. GPC ($CHCl_3$; polystyrene standard): M_n = 6300 (calcd for P_n = 22, M_n = 8262), M_w = 7200.

Poly(*N*-[4-(heptyloxy)-3-[(*S*)-(1-methylheptyl)oxy]benzoyl]ethylenimine) (LPEI(22)-3*,4/7). Anal. Calcd for $(C_{24}H_{39}NO_3)_n$ (corresponding to a 100% substitution; $M_{rep.unit}$ = 389.58): C, 73.99; H, 10.09; N, 3.60 (C/N = 20.55). Found: C, 72.95; H, 10.31; N, 3.52 (C/N = 20.72). Degree of substitu-

tion calculated from C/N ratio, >95%. GPC ($CHCl_3$; polystyrene standard): M_n = 5700 (calcd for P_n = 22, M_n = 8571), M_w = 6600.

For the synthesis of statistical copolymers, a homogeneous mixture of substituted benzoyl chlorides was used which was obtained by mixing the corresponding benzoic acids in the desired stoichiometric ratio before the conversion into acid chlorides.

Poly[(*N*-[3,4,5-tris(decyloxy)benzoyl]ethylenimine)-*co*-(*N*-[4-(decyloxy)benzoyl]ethylenimine)] (LPEI(22)-Co4/3,4,5). The reaction was performed with a 2:1 stoichiometric mixture (excess of the single-chain benzoyl chloride needed) of the corresponding acid chlorides. The ^{1}H NMR spectrum is equivalent to that of a mixture of **LPEI(22)-4** and **LPEI-(22)-3,4,5**. Comonomer composition in the resulting copolymer according to ^{1}H NMR (determined from aromatic protons) was ~1:1. Anal. Calcd for $(C_{29}H_{49}NO_3)_n$ (corresponding to a 100% substitution and a 1:1 comonomer ratio; $M_{rep.unit}$ = 459.72): C, 75.77; H, 10.74; N, 3.05 (C/N = 24.84). Found: C, 75.12; H, 11.00; N, 3.30 (C/N = 22.76). Degree of substitution calculated from C/N ratio, ~91%. GPC (THF; polystyrene standard): M_n = 8200 (calcd for P_n = 22, 100% substitution, M_n = 10 114), M_w = 14 100.

Poly[(*N*-[4-(heptyloxy)-3-[(*S*)-(1-methylheptyl)oxy]benzoyl]ethylenimine)-*co*-(*N*-[3,4-bis(heptyloxy)benzoyl]ethylenimine)] (LPEI(22)-Co3*,4/7). The ^{1}H NMR spectrum is equivalent to that of poly(*N*-[3,4-bis(heptyloxy)benzoyl]-ethylenimine); additionally, the signal for the proton on the chiral center ($C_6H_{13}CH(CH_3)OAr$) is observed as a weak, broad signal at 4.25 ppm. Anal. Calcd for $(C_{23.1}H_{37.2}NO_3)_n$ (corresponding to a 100% substitution; $M_{rep.unit}$ = 376.96): C, 73.60; H, 9.95; N, 3.72 (C/N = 19.78). Found: C, 72.86; H, 9.79; N, 3.60 (C/N = 20.24). Degree of substitution calculated from C/N ratio, >95%. GPC ($CHCl_3$; polystyrene standard): M_n = 5800 (calcd for P_n = 22, M_n = 8293), M_w = 6700.

Chiral poly(1-methylethylenimine) was obtained by acid hydrolysis of poly(*N*-acetyl-1-methylethylenimine), which was synthesized by bulk cationic ring-opening polymerization of 2,4-dimethyl-2-oxazoline according to a literature procedure[48] but using ethyl trifluoromethanesulfonate as initiator. The monomer was synthesized from acetonitrile and (*S*)-2-amino-1-propanol (Aldrich) according to the general method described by Witte and Seeliger[49] for the preparation of oxazolines from the corresponding nitriles using cadmium acetate as a catalyst.

(*S*)-2,4-Dimethyl-2-oxazoline. (*S*)-2-Amino-1-propanol (10 g, 0.135 mol) was added dropwise to a stirred mixture of (acetonitrile 7.2 g, 6.7 mL, 0.175 mol) and cadmium acetate dihydrate (330 mg, 1.24 mmol) at 70 °C. After complete addition, the reaction is heated to 100 °C and stirred overnight under an argon atmosphere. The reaction mixture is distilled to give a crude product (bp ≈ 110 °C), which still contains considerable amounts of starting material. The monomer is obtained pure by repeated distillation over ion-exchange resin (Amberlite IRC-50) under reduced pressure at room temperature and collected in a trap cooled to −78 °C: yield 5.3 g (40%); ^{1}H NMR ($CDCl_3$, 200 MHz) δ 1.17 (d, 3H, C*H*$_3$CH), 1.89 (s, 3H, C*H*$_3$C=N), 3.68 (dd, 1H, NCH(CH$_3$)C*H*HO), 4.06 (m, 1H, NC*H*(CH$_3$)CHHO), 4.26 (dd, 1H, NCH(CH$_3$)CH*H*O); mass spectrum, *m*/*e* 99.1. Anal. Calcd for C_5H_9NO (M_r = 99.07): C, 60.58; H, 9.15; N, 14.13. Found: C, 59.56; H, 8.91; N, 14.50.

Poly(*N*-acetyl-(*S*)-1-methylethylenimine). (*S*)-2,4-Dimethyl-2-oxazoline (4.2 g, 42 mmol) and ethyl trifluoromethanesulfonate (87 mg, 63 μL, 0.49 mmol, 0.0117 equiv) were heated to 90 °C in a sealed tube. After 6 h, the temperature was increased to 110 °C, and the polymerization proceeded for an additional 3 days. The crude polymer was dissolved in acetonitrile and precipitated in petroleum ether. This procedure was repeated twice to give a pale yellow, waxy hygroscopic solid: yield 1.6 g (38%); ^{1}H NMR ($CDCl_3$, 200 MHz) δ 1.05−1.50 (br, 3H, C*H*$_3$CH), 1.95−2.35 (br, 3H, C(O)C*H*$_3$), 2.93−4.70 (m, 3H, C*H*NC*H*$_2$).

Poly((*S*)-1-methylethylenimine). Poly(*N*-acetyl-(*S*)-1-methylethylenimine) (600 mg) was heated to reflux in 8 N aqueous HCl solution (70 mL) for 9 days. After cooling, the solution was brought to pH 10 by the addition of aqueous NaOH, the resulting yellow solution was extracted several times with dichloromethane, and the combined organic layers were dried with sodium sulfate. After evaporation of the dichloromethane, the residue was dried in vacuo to yield 270 mg of a yellow viscous oil: ^{1}H NMR ($CDCl_3$, 200 MHz) δ 0.8−1.2 (br, 3H, C*H*$_3$CH), 1.55−2.05 (br, 1 H, N*H*), 2.30−2.70 (m, 3H, C*H*NHC*H*$_2$).

Alternatively, the polymer may be isolated as the hydrochloride to avoid the extensive extraction step. In this case, the hydrochloric acid as well as the formed acetic acid is distilled azeotropically from the reaction mixture with occasional addition of 20 mL portions of water (total amount, ~150 mL). The solvent is removed and the residue dried in vacuo to give a pale yellow solid: ^{1}H NMR (D_2O, 200 MHz) 1.1−1.4 (d, 3H, C*H*$_3$CH), 3.0−3.7 (m, 3H, C*H*NC*H*$_2$), 4.2−4.6 (br, N*H*$_2^+$ exchanged with *H*DO, 4.8 ppm).

Poly(*N*-[3,4-bis(decyloxy)benzoyl]-(*S*)-1-methylethylenimine) (ChPEI(30)-3,4). Poly((*S*)-1-methylethylenimine) (263 mg, 4.6 mmol), 3,4-bis(decyloxy)benzoyl chloride (2.7 g, 6 mmol), and DMAP (750 mg, 6.2 mmol) were heated to 70 °C in absolute DMF under an argon atmosphere. After 3 days, the solvent was removed and the residue dried under vacuum for 1 day. The brownish solid was dissolved in 50 mL of dichloromethane and successively washed with 100 mL portions of 1 N NaOH (twofold) and three times with water. The solvent was removed and the residue repeatedly washed with cold acetone (purity checked by TLC). The resulting yellow oil was freeze-dried from benzene to give 1.02 g (47%) of a white powder: ^{1}H NMR (200 MHz, $CDCl_3$) δ 0.86 (t, 6H, C*H*$_3$-(CH$_2$)$_9$O), 1.15−1.50 (br, 28H, CH$_3$(C*H*$_2$)$_7$CH$_2$CH$_2$O), 1.55−1.70 (br, 3H, CH$_2$NC(C*H*$_3$)H), 1.60−1.90 (br, 4H, CH$_3$(CH$_2$)$_7$C*H*$_2$-CH$_2$O), 3.70−4.10 (br, 7H, C*H*$_2$NC(CH$_3$)*H* and CH$_3$(CH$_2$)$_8$C*H*$_2$O), 6.5−7.0 (br, 4H, Ar H-2,5,6). Anal. Calcd for $(C_{30}H_{51}NO_3)_n$ (corresponding to a 100% substitution; $M_{rep.unit}$ = 473.74): C, 76.06; H, 10.85; N, 2.96 (C/N = 25.70). Found: C, 76.45; H, 11.67; N, 3.47 (C/N = 22.03). Degree of substitution calculated from C/N ratio, 84%. GPC (THF; polystyrene standard): M_n = 15 800 (corresponding to $P_n \approx 30$), M_w = 21 500.

Acylation of Branched Poly(ethylenimine) with 3,4-Bis(decyloxy) chloride. The polymer analogous conversion of branched poly(ethylenimine)s was performed according to the following general procedure for **BPEI(20)-3,4**. The index *n* in the term **BPEI(*n*)-3,4** refers to the approximate number of amino units in the starting material: $n \approx x(E) + y(E) + z(E)$.

Branched poly(ethylenimine) (72 mg, ~1.55 mmol of primary and secondary amino units) was stirred under argon with 3,4-bis(decyloxy)benzoyl chloride (800 mg, 1.77 mmol) and DMAP (224 mg, 1.83 mmol) at 70 °C for 3 days. The DMF was removed by distillation and the residue dissolved in dichloromethane. The organic solution was washed with water three times, dried with Na_2SO_4, and concentrated by removing most of the solvent. After filtration through a micrometer-size filter, the polymer was precipitated in acetone and freeze-dried from benzene to yield 285 mg of a pale yellow solid: ^{1}H NMR (200 MHz, $CDCl_3$) δ 0.86 (t, C*H*$_3$), 1.1−1.6 (br, CH$_3$(C*H*$_2$)$_7$-CH$_2$CH$_2$O), 1.5−1.9 (br, C*H*$_2$CH$_2$O), 2.2−2.9 (m, C*H*$_2$NH of residuing amino groups), 3.2−4.0 (br, C*H*$_2$NC(=O) and C*H*$_2$-OAr), 6.4−7.0 (br, Ar H-2,5,6 of tertiary amides and Ar H-2 of secondary amides), 7.1−7.5 (Ar H-2,6 of secondary amides and N*H*-CO).

Characterization of Synthesized Branched Poly(ethylenimine)s. BPEI(10)-3,4. The ratio of primary/secondary/tertiary amino groups in starting material (information provided by manufacturer, BASF AG, Ludwigshafen, Germany) was 44:38:18. Anal. Calcd for $(C_{24.1}H_{41.1}NO_{2.5})_n$ (corresponding to a 100% substitution of the primary and secondary amino groups; $M_{rep.unit}$ = 384.90): C, 75.21; H, 10.76; N, 3.64 (C/N = 20.66). Found: C, 74.24; H, 11.03; N, 3.75 (C/N = 19.81). Degree of substitution calculated from C/N ratio, >94%. GPC ($CHCl_3$; polystyrene standard): M_n = 2900 (calcd for P_n = 10, M_n = 3849), M_w = 3800.

BPEI(20)-3,4. The ratio of primary/secondary/tertiary amino groups in starting material (information provided by manufacturer, BASF AG) was 40:35:25. Anal. Calcd for $(C_{22.3}H_{38}NO_{2.3})_n$ (corresponding to a 100% substitution of the primary and secondary amino groups; $M_{rep.unit}$ = 356.96): C,

75.04; H, 10.73; N, 3.92 (C/N = 19.14). Found: C, 73.66; H, 10.83; N, 3.69 (C/N = 19.96). Degree of substitution calculated from C/N ratio, >95%. GPC ($CHCl_3$; polystyrene standard): M_n = 4200 (calcd for P_n = 20, M_n = 7139), M_w = 6600.

BPEI(230)-3,4. The ratio of primary/secondary/tertiary amino groups in starting material was 25:50:25.[50−52] Anal. Calcd for $(C_{22.3}H_{38}NO_{2.3})_n$ (corresponding to a 100% substitution of the primary and secondary amino groups; $M_{rep.unit}$ = 356.96): C, 75.04; H, 10.73; N, 3.92 (C/N = 19.14). Found: C, 71.77; H, 10.78; N, 4.74 (C/N = 15.14). Degree of substitution calculated from C/N ratio, 77%. A portion of residuing unsubstituted amino groups in product was not calculated due to very broad ^{1}H NMR signals. GPC ($CHCl_3$; polystyrene standard): M_n = 61 000 (calcd for P_n = 230, M_n = 82 101), M_w = 128 000.

Characterization of Thermal Behavior and Structural Analysis. Polarizing microscopy studies were performed with an Ortholux II POL-BK polarizing microscope (Leitz). The temperature was controlled on a FP 52 heating stage with an FP 5 (Mettler 9) control unit. Photographs of the microscopic textures were taken with an Olympus SC 35 (Type 12) camera and Kodak-Ektachrome 400 ASA films. DSC measurements were carried out on a microcalorimeter DSC-7 (Perkin-Elmer). Portions of 3−10 mg of the compounds were sealed in small aluminum pans. Data acquisition and analysis were performed with an Epson PC using the Perkin-Elmer Multitasking software. Indium and lead standards were used for calibration. If not otherwise noted, all transition temperatures given in the text were taken from the peak minima of the first cooling (monotropic mesophases) and the peak maxima of the second DSC heating trace (scan rate, 10 °C min^{-1}). Glass transition temperatures were taken from the inflection points of the curves.

X-ray investigations of the liquid crystalline phases were carried out using Cu Kα radiation (λ = 1.541 nm), monochromized by a flat graphite monochromator and a Siemens X-1000 area detector device or a flat film camera operating in vacuum using different sample detector distances. Oriented samples were prepared by pulling fibers out of a melt. The sample temperature was maintained with a Linkam THM 600 hot stage and controller with an accuracy of 0.1 K. Scattering intensities in the X-ray diffractograms are shown in relation to the scattering vector Q (Å^{-1}) with $Q = 2\pi \sin\theta/\lambda$. The X-ray structural analysis of ethyl 4-(heptyloxy)-3-hydroxybenzoate was performed using an Enraf-Nonius CAD 4.

Results and Discussion

Liquid Crystalline Open-Chain Oligoamides. In the case of ethylenediamine as the simplest open-chain "oligoamine", the formation of a hexagonal columnar phase was described by Percec *et al.*[19] by the use of 3,4,5-trialkoxybenzoyl units with linear alkyl chains of at least 10 carbon atoms. The bisamides form semicolumns which are stabilized by intermolecular hydrogen bonds along the column axis. The columnar unit of the hexagonal mesophase is constituted by two such independent semicolumns. The formation of a monotropic mesophase by 3,4-dialkoxybenzoyl derivatives of the higher homologue diethylenetriamine with an alkyl chain length of 6−12 carbon atoms was described by Lattermann *et al.*[42] Therefore, the ability of the *N*-acylated oligoamines to form mesomorphic phases is preserved even after the ring is opened and the intrinsic disklike structure of the molecules is lost. The higher conformational flexibility compared to the macrocyclic derivatives, however, leads to a metastability of the phases. Contrary to a recent publication,[43] where a narrow enantiotropic mesophase was described for the corresponding substituted triethylenetetraamine, we could only find a metastable mesophase for both the 3,4-bis(decyloxy)benzoyl derivatives of triethylenetetraamine **N(4)-3,4** and tetraethylenepentaamine **N(5)-3,4** (Figure 2).

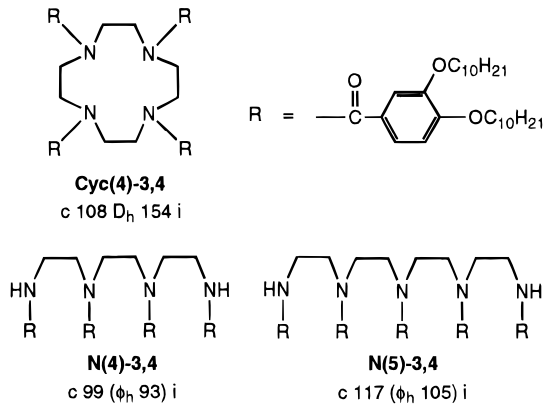

Figure 2. Phase behavior of cyclic and linear oligoamides: c, crystalline; D_h, discotic hexagonal mesophase; ϕ_h, hexagonal columnar mesophase; i, isotropic. Phase transition temperatures are given in °C.

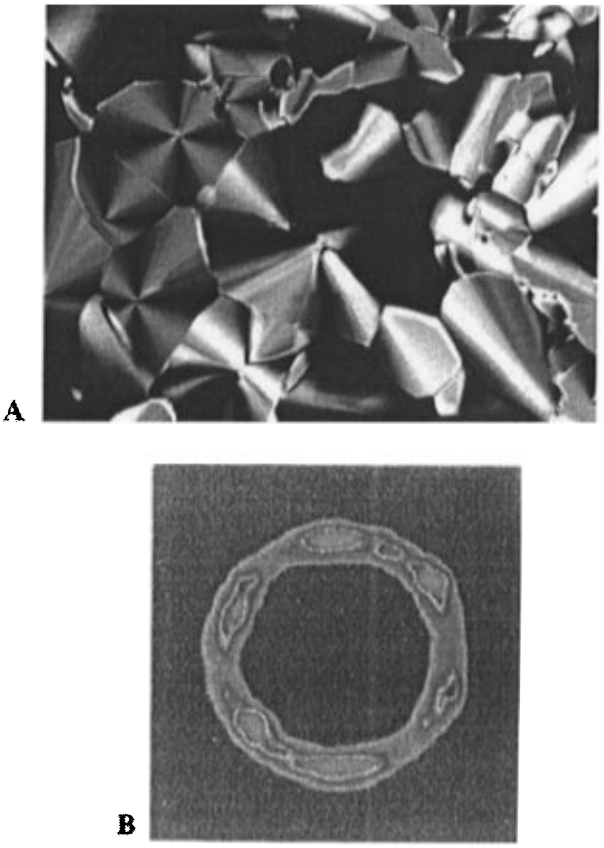

Figure 3. (A) Texture of the open-chain oligoamide **N(5)-3,4** (T = 104 °C; cooling from the isotropic state by 2 °C min^{-1}). (B) Flat camera photograph (small-angle region) of an oriented sample at room temperature obtained by quickly cooling from the mesophase.

Whereas a hexagonal columnar arrangement could be unambiguously demonstrated for the cyclic tetramer **Cyc(4)-3,4** by the X-ray pattern of a magnetically oriented monodomain,[40] the mesophase structure of the open-chain oligomers is still under discussion.[40,42] The microscopic texture of **N(5)-3,4** in the mesophase shown in Figure 3A consists of *focal conic* structures next to distinct homeotropic regions and is thus of high similarity with the textures found for macrocyclic oligoamides.

For the characterization of the mesophase by X-ray diffraction, **N(5)-3,4** was cooled from the isotropic state into the mesophase in the presence of a magnetic field of ∼0.8 T, oriented perpendicular to the capillary axis, and finally supercooled to room temperature. The X-ray

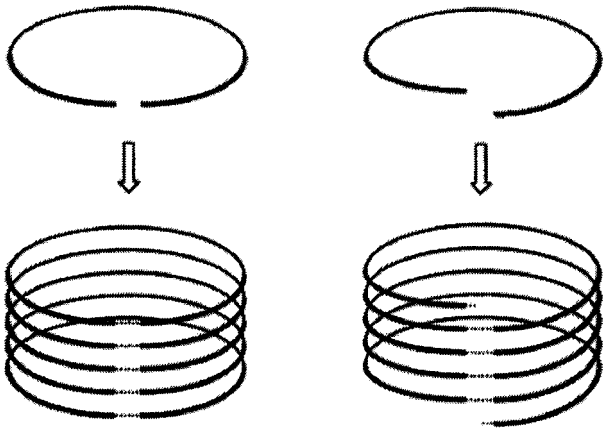

Figure 4. Formation of columnar aggregates by intramolecular or intermolecular hydrogen bonds.

flat plate graph of an oriented sample in Figure 3B shows a distinct hexagonal diffraction pattern which, although slightly distorted, clearly proves the hexagonal columnar structure of the frozen monotropic mesophase at room temperature. In the wide-angle region (not shown), only a nonoriented halo is found, so that a possible crystallization during the preparation of the sample can be excluded. In the case of **N(4)-3,4**, the hexagonal mesophase structure was proven by a (110) reflection, which was found in the characteristic ratio of $1:3^{1/2}$ compared to the first-order peak. Both linear oligoamides **N(4)-3,4** and **N(5)-3,4** therefore show the same mesophase structure as the macrocyclic derivatives. Considering the relatively high experimental error of the flat camera picture, no exact lattice parameters may be given. Nevertheless, there is no evidence for an expansion of the hexagonal lattice with increasing chain length; both oligoamides show approximately the same intercolumnar distance.

In macrocyclic oligoamides, the cyclic structure is given by the discoid molecular geometry. In the open-chain oligoamides, this geometry can perhaps be achieved by means of intramolecular hydrogen bonding between terminal amide groups. These cyclic subunits are then stacked into a columnar arrangement. Alternatively, the formation of intermolecular hydrogen bonds between the oligomeric subunits may be considered: the column would then be formed by a helically folded chain of hydrogen-bonded oligoamide molecules. The latter possibility would easily explain the comparable lattice parameters of both compounds. Figure 4 illustrates the two possible mechanisms for the formation of columnar structures by linear *N*-acylated oligoamines.

An increase of the chain length into the polymeric region should decrease the probability of intramolecular hydrogen bonding. In a system governed by intermolecular hydrogen bonding, however, the hydrogen bonds within the columnar aggregates would be partially substituted by covalent bonds. For this latter case, an extreme stabilization of the columnar arrangement was expected. This will be discussed in the next section.

Linear Polyamides. The polymer analogues of the open-chain oligoamides were synthesized by polymer analogous reaction of linear poly(ethylenimine)s of different degrees of polymerization ($n = 11, 22, 51, 186$) with 3,4-bis(decyloxy)benzoyl chloride and DMAP as base in DMF solution (Scheme 1).[40]

Nearly complete substitution of the amino groups was determined from ^{1}H NMR spectroscopy and elemental analysis (see Experimental Section). Considering the

Scheme 1

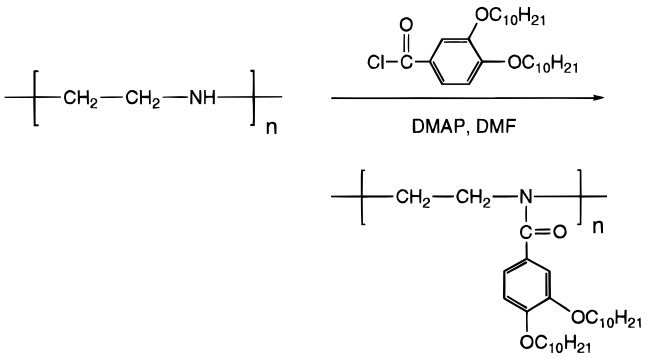

experimental error of these methods, a polymer analogous conversion of higher than 95% can be assumed. In the ^{1}H NMR spectra of the poly(ethylenimine) derivatives **LPEI(*n*)-3,4** the nonreacted amino groups can be seen only as a very broad peak of low intensity at $\delta =$ 2.85 ppm. The GPC eluogram of the compounds shows a narrow weight distribution of these systems, which on the one hand is due to the homogeneity (low polydispersity) of the starting polymers prepared by cationic polymerization, and on the other hand points to the uniformity of the polymer analogous acylation process.

All synthesized polyamides with the 3,4-bis(decyloxy) side group form enantiotropic liquid crystalline phases. The monotropic mesophase found in low molecular weight oligoamides is therefore stabilized in polymeric systems. In microscopic investigations, the formation of a *fan-shaped* texture with homeotropic regions was observed after slow cooling from the isotropic melt.[40] The same texture as shown for the oligomer **N(5)-3,4** in Figure 3A is characteristic also for all polymers **LPEI(*n*)-3,4**, with the exception of **LPEI(186)-3,4**, where only an uncharacteristic texture is observed due to the high molecular weight (in general, the domain size decreases with increasing chain length). DSC thermograms of all polymers show a glass transition at ~60 °C and first-order transitions from the liquid crystalline to the isotropic state between 99 and 127 °C, depending on the molecular weight. Considering the polymeric nature of the compounds, only a slight undercooling of the transition to the isotropic is observed (6−13 °C). The corresponding clearing enthalpy of 1.1−1.2 kJ mol^{-1} (per repeating unit) is a little below those of the comparable azacrown derivatives; the macrocyclic model compound **Cyc(4)-3,4** gives a value of 6.7 kJ mol^{-1}, or 1.68 kJ mol^{-1} per ethyleneamine unit.

At room temperature, the polymers are anisotropic glasses which—at least in the case of low molecular weights—slowly crystallize: after keeping an amorphous sample of **LPEI(22)-3,4** at room temperature for 6 months, the melting of crystalline domains was observed in the first DSC heating scan (g, 58 °C; c, 69 °C; ϕ_h, 120 °C i) and in the following heating cycles was no longer detected (Table 1). In addition, for the higher molecular weight samples ($n \approx 22, 51, 186$), an additional signal at 80−90 °C was found which, after annealing the samples for 3 days just above the glass transition (65 °C), could be identified as a broad first-order transition. The dependence of this transition on the history of the sample points to the melting of crystalline domains which are not identical with the crystalline domains formed at room temperature: after annealing **LPEI(51)-3,4** at 65 °C, two peaks at 59 and 98 °C were found, and the glass transition disappeared. Although less pronounced, the same behavior is found for **LPEI(22)-**

Table 1. Thermal Phase Transition Temperatures Depending on the Thermal History of the Samples[a]

	DSC scan	*T* (°C)
LPEI(22)−3,4	second heating	g, 61; ϕ_h, 120 i
	first cooling	g, 55; ϕ_h, 109 i
	heating after storing at room temperature for 6 months	g, 67; ϕ_h, 120 i
	heating after annealing at 65 °C for 2 days	c_1, 62; c_2, 88; ϕ_h, 119 i
LPEI(51)−3,4	second heating	g, 63; ϕ_h, 125 i
	first cooling	g, 58; ϕ_h, 115 i
	heating after annealing at 65 °C for 2 days	c_1, 59; c_2, 98; ϕ_h, 124 i

[a] Given in °C, taken from DSC thermograms; heating and cooling rate, 10 °C min^{-1}. c, crystalline; g, glassy; ϕ_h, hexagonal columnar mesophase; i, isotropic.

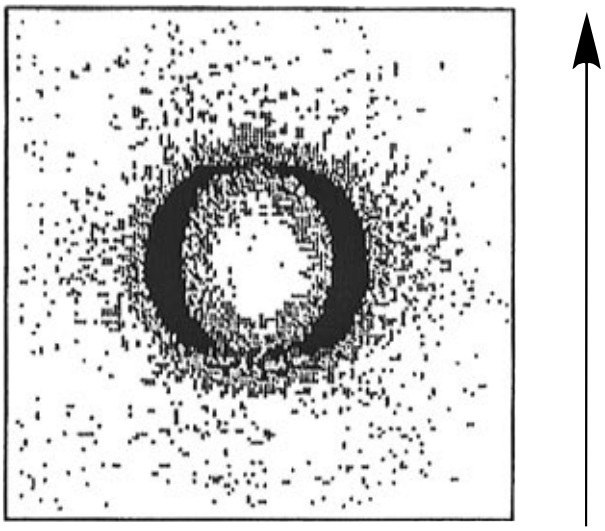

Figure 5. Flat camera photograph (small-angle region) of an oriented fiber of **LPEI(186)-3,4** drawn in the mesophase. The arrow indicates the fiber direction.

3,4. In the following heating and cooling scans, the original behavior of a nonannealed sample was found with clearing temperatures and clearing enthalpies independent of the history of the sample. The observed transition temperatures are listed in Table 1. Decomposition of the polymers due to the annealing process can therefore be excluded.

In the X-ray diffraction pattern in the mesophase of **LPEI(22)-3,4** we found three maxima in the low-angle region, the corresponding layer spacings of which are in the ratio of $1:1/3^{1/2}:1/2$.[40] Therefore, the three peaks could be assigned to the (100), (110), and (200) reflections (corresponding distances were 30.97, 17.83, and 15.50 Å, respectively) of a hexagonal columnar arrangement. As in the case of the comparable azacrown derivatives, the mixed as well as the second-order reflections were of very low intensity compared to the first-order reflections. The halo in the wide-angle region was characteristic for only short-range ordered alkyl chains corresponding to an intermediate distance of 4.7 Å. The hexagonal lattice parameter, i.e., the intercolumnar distance, could be calculated from the (100) reflection as 35.8 Å and was thus above the value for the macrocyclic model compound **Cyc(4)-3,4** (33.2 Å).

The higher molecular weight polymers **LPEI(51)-3,4** and **LPEI(186)-3,4** give the same X-ray pattern, with the intercolumnar distance being independent of the molecular weight. In addition, by stretching within the mesophase, an orientation of the polymers can be achieved. The small-angle X-ray pattern obtained from an oriented fiber of **LPEI(186)-3,4** is illustrated in Figure 5. As in the case of low molecular weight discotics, the first-order reflection is split perpendicular to the shear director;[53,54] thus, with mechanical stress,

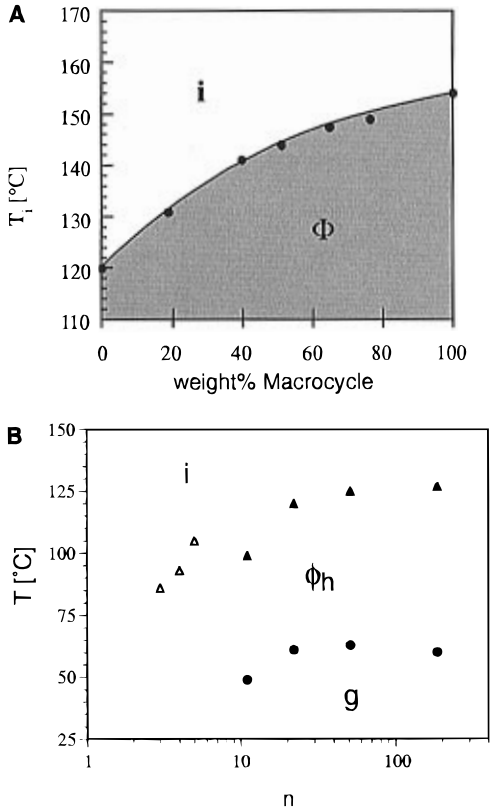

Figure 6. (A) Mixtures of linear polyamide **LPEI(22)-3,4** with macrocycle **Cyc(4)-3,4**: clearing temperature depending on macrocycle content. (B) Phase behavior of linear oligo- and polyamides as a function of the degree of polymerization. For the monotropic *N*-acylated oligoamides, only the temperatures of the transition from the isotropic to the metastable mesophase as observed in the DSC cooling scans are shown.

the columns are oriented along the shear axis. The orientability increases with molecular weight: no fiber could be drawn from **LPEI(22)-3,4**, whereas the polymers **LPEI(51)-3,4** and **LPEI(186)-3,4** are easily aligned by mechanical stress. The wide-angle halo (not shown here) also exhibits a slight orientation in shear direction, which is probably caused by the less mobile alkyl segments in the direct neighborhood of the column center.

To prove the identity of the mesophase structures found for the linear oligoamide **N(5)-3,4**, the macrocycle **Cyc(4)-3,4**, and the polymer **LPEI(22)-3,4**, their miscibility in the liquid crystalline state was investigated in contact preparations under the polarizing microscope. All compounds are miscible over the whole concentration range within the mesophase. For example, the clearing temperature of the binary system macrocycle/polymer increases with the amount of macrocycle in the mixture (Figure 6A). Again, typical *fan-shaped* textures are observed under the polarizing microscope within the mesophase.

Table 2. Phase Behavior of *N*-Acylated Linear Polymers LPEI(*n*)−3,4[a]

n	phase behavior	$\Delta H_{1c\rightarrow i}$
11 [**LPEI(11)−3,4**]	g, 49; ϕ_h, 99 i	1.1
22 [**LPEI(22)−3,4**]	g, 61; ϕ_h, 120 i	1.2
51 [**LPEI(51)−3,4**]	g, 63; ϕ_h, 125 i	1.2
186 [**LPEI(186)−3,4**]	g, 60; ϕ_h, 127 i	1.2

[a] g, glassy; ϕ_h, hexagonal columnar mesophase; i, isotropic; phase transition temperatures given in °C, isotropization enthalpies $\Delta H_{1c\rightarrow i}$ in kJ mol^{-1} rep.unit^{-1} (taken from the second DSC heating scan, heating rate, 10 °C min^{-1}).

The dependence of the thermal phase behavior of the polymers **LPEI(*n*)-3,4** on the polymer chain length is listed in Table 2 and graphically summarized in Figure 6B. Phase transition temperatures (taken from the first DSC cooling scan) of the monotropic oligoamides **N(4)-3,4** and **N(5)-3,4** and of the homologous diethylenetriamine derivative (named in this context as **"N(3)-3,4"**) synthesized by Lattermann *et al.*[42] are included.

The elongation of the polymer chain stabilizes the monotropic mesophase found in the oligomeric region. Above $n \approx 22$, the clearing temperatures are nearly independent of the molecular weight. For a polymer chain of approximately 186 repeating units, the clearing temperature is increased by only 7 °C compared to that of **LPEI(22)-3,4**. Possibly, the formation of a columnar structure is disturbed by a higher number of disordered, coiled main-chain segments, and the clearing temperature is thus limited.

The observed difference between the polymeric materials and the defined low molecular weight samples may be due to a possible influence of the molecular weight distribution on the phase behavior. In particular, the clearing temperature of the enantiotropic **LPEI-(11)-3,4** lies slightly below the transition from the isotropic state to the mesophase of the monotropic oligoamide **N(5)-3,4**. During several reprecipitation steps of this polymer from dichloromethane solution in acetone, different clearing temperatures from 99 to 106 °C were measured. Obviously, **LPEI(11)-3,4** lies in a range where small deviations in the molecular weight have a drastic effect on the transition temperatures. For all other polymers, reprecipitation did not influence the clearing point significantly.

The phase behavior of oligomeric and polymeric compounds shows that the formation of hexagonal columnar mesophases by acylated amines is not restricted to molecules with an intrinsic discoid structure: macrocyclic and open-chain oligomers as well as linear polymers form a hexagonal columnar structure. Two mechanisms for the formation of columnar units from linear oligoamides were discussed above (Figure 4). A discoid molecular conformation would be provided by intramolecular hydrogen bonding; the columns are then formed by stacking the molecular disks. On the other hand, the columns may be formed by intermolecular hydrogen bonds between single, helically twisted oligoamide molecules. The stabilization of the monotropic mesophase at higher molecular weights, especially in polymeric materials, supports the latter explanation. Covalent bonds as well as the existence of different chain lengths stabilize the aggregation of the subunits in longer main chains by replacing the weaker hydrogen bonds, support the mesophase formation, and suppress crystallization.

At this stage of the discussion, it should be noted that a columnar arrangement may also be formed by a more or less stretched polymer chain radially surrounded by

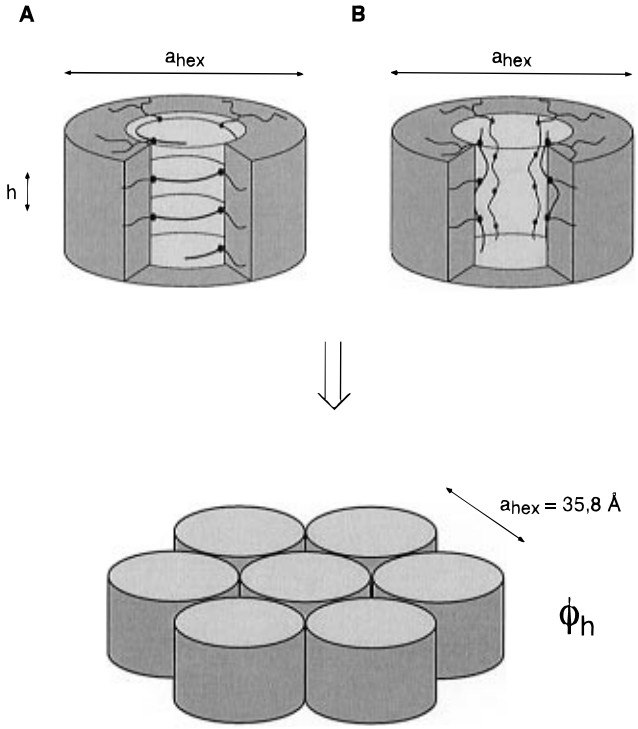

Figure 7. Formation of a hexagonal columnar mesophase based on columnar units formed by (A) a single polymer chain and (B) several stretched polymer chains.

alkyl side chains. Such a structure would be comparable with those found in mesomorphic poly(alkylsilane)s, which in certain cases indeed form hexagonal mesophases.[29,30] In the case of a stretched polymer main chain, however, the higher measured intercolumnar distance compared to that of macrocyclic oligoamides can only be explained if one column is formed by two or more polymer chains, as indicated in Figure 7B. The cooperative packing of several polymer chains, however, would afford a much higher order than a single, more or less helically folded chain (Figure 7A). In this context, the column diameter may be guessed from the relation $\rho = M_r/\{(3/2)^{1/2} a_{hex}^2 h N_A\}$, with ρ as the density, the molecular weight per repeating unit M_r, the Avogadro number N_A, the hexagonal lattice parameter a_{hex} representing the intercolumnar distance, and h as the intracolumnar distance. Considering the identities of the mesophase structure, of the chemical structure of the repeating units, and of the determined average distances of the alkyl side chains, it seems reasonable to assume nearly the same values for the denstity ρ and for the intracolumnar distance h in the mesophases of both the macrocylic oligoamide **Cyc(4)-3,4** and the linear polyamide **LPEI(22)-3,4**. With this simplification, the column area in the polymeric mesophase is calculated from the hexagonal lattice parameters to be formed by four or five *N*-3,4-bis(decyloxy)-benzoylated ethyleneamine units.

In the moment, we cannot experimentally distinguish between the two possibilities. Nevertheless, the structural similarity of macrocyclic and polymeric acylated amines as well as their perfect miscibility in the mesophase, to our understanding, point to a single, helically folded main chain which is surrounded radially by the alkyl side chains, adopting a shape similar to *hairy rod* systems.[55] Figure 8 shows the CPK models of such a mesomorphic *N*-acylated poly(ethylenimine) with a helical main chain conformation.

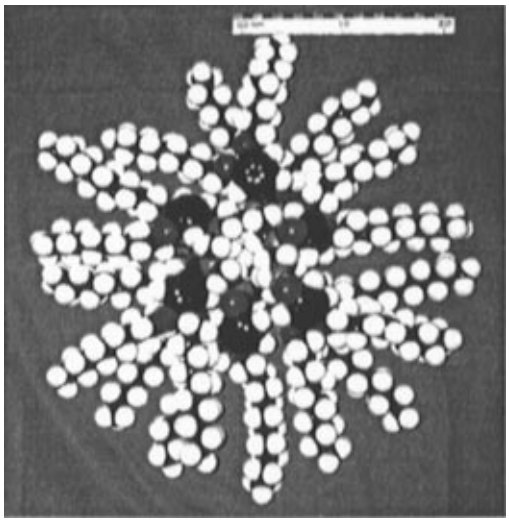

Figure 8. CPK model of an *N*-acylated poly(ethylenimine), **LPEI(*n*)-3,4**.

In this respect, the system describes an intermediate situation between the observed hexagonal columnar mesophases in long alkyl chain-substituted, helical poly(L-glutamate)s[28] and polymeric derivatives with tapered side groups described by Percec *et al.*[19,26] In the first case of the synthetic polypeptides, a pre-existing helical polymeric chain is merely radially substituted by the aliphatic side chains. In the latter materials, on the other hand, the polymer main chain is not directly fixed to the formanisotropic units but is separated via a flexible spacer, thus not necessarily adopting a regular conformation. Nevertheless, based on molecular modeling calculations, a helical chain conformation has been discussed which is favored by the packing of the tapered side groups.[27] It is thus understandable that, in the case of the substituted poly(ethylenimine)s discussed here, the direct linkage of the alkyl side groups by a stiff amide bond may enforce an overall rigid helical structure.

It should be noted that the observed hexagonal columnar arrangement is in striking contrast to the structures usually observed in acylated linear poly(ethylenimine)s: in *N*-alkanoyl- or *N*-toluoyl-substituted linear poly(ethylenmine)s, the side groups are aligned in an alternating manner along the main chain (herringbone structure) and thus form a lamellar crystal.[56] This tendency was already used for the synthesis of calamitic liquid crystalline side-chain polymers with smectic phases;[57] hexagonal columnar structures are not known for acylated poly(ethylenimine)s so far, and their appearance in the described polymers may be seen as a direct consequence of the side groups. For the sake of completeness, however, it should be mentioned that helical structures already have been found in anhydrous linear poly(ethylenimine), which, according to X-ray studies, exists as double-stranded helical chains. The unsubstituted linear polymer has hygroscopic properties and is readily transformed to the linear structure by absorption of water.[58,59] As a reference system for the described polyamide, however, the lamellar *N*-benzoylated poly(ethylenimine) mentioned above has to be considered.[56]

Variation of the Side-Chain Structure. In the case of *N*-acylated tetraazamacrocycles, discotic mesomorphism was observed only for 3,4-dialkoxybenzoyl derivatives.[39] Derivatives with a pendant isomeric 3,5-dialkoxybenzoyl side group as well as such containing

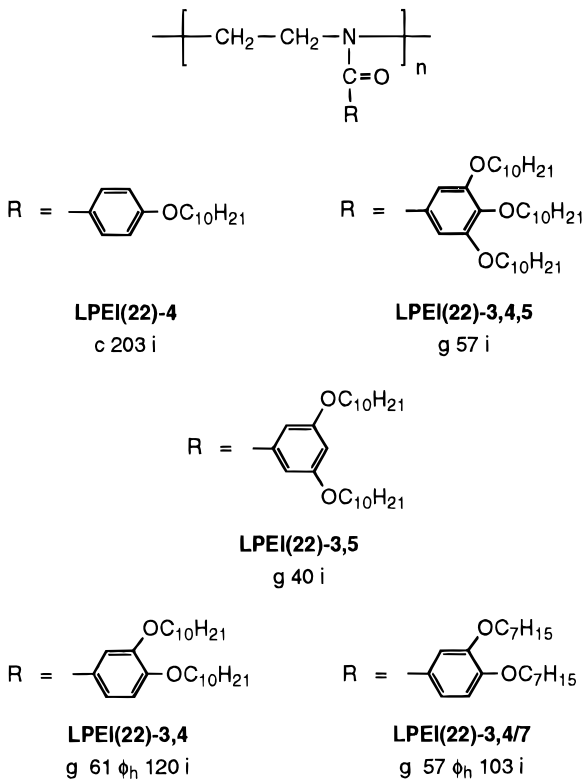

Figure 9. Phase behavior of *N*-acylated poly(ethylenimine)s: g, glassy; c, crystalline; ϕ_h, hexagonal columnar mesophase; i, isotropic. Transition temperatures are given in °C. In the first DSC heating curve of **LPEI(22)-4**, two additional first-order transitions at 64 and 75 °C are detected, whereas in the second heating scan, only the latter can be observed. These transitions presumably correspond to changes between different crystalline modifications.

the 3,4,5-trialkoxybenzoyl unit are glassy, whereas the single-chain substituents constituted from 4-alkoxybenzoic acid lead to crystalline materials.[38,60] A similar characteristics is found in the series of linear polyamides (Figure 9). The linear poly(ethylenimine) **LPEI(22)-3,4,5** is an isotropic glass at room temperature, and in the DSC measurements, only a glass transition at 57 °C is observed. The polymer **LPEI(22)-4** substituted with only one chain per repeating unit is highly crystalline and melts at 203 °C.

The degree of substitution achieved in the polymer analogous acylation reaction is only about 80% for the three-chain-substituted poly(ethylenimine), which is probably due to the increased steric requirements of the side groups. Even after reacting an 80% substituted polymer with additional acid chloride for several days, no further acylation was detected. Reserving further X-ray investigations for the 4-(decyloxy)benzoyl derivative **LPEI(22)-4**, we assume a lamellar crystal structure in accordance with the literature-described herringbone structures found for toluoyl- and 4-chlorobenzoyl derivatives of poly(ethylenimine).[56] On the other hand, the amorphous character of **LPEI(22)-3,4,5** may be seen as a consequence of the high density of alkyl side chains, which allows neither the formation of a possibly lamellar crystal nor a helically folded conformation of the main chain in a columnar arrangement.

Two additional polymers were synthesized that possess the same side-chain density as the liquid crystalline homopolymer **LPEI(*n*)-3,4**: the two-chain isomer **LPEI(22)-3,5** as well as a statistical copolymer **LPEI(22)-Co4/3,4,5** bearing 4-(decyloxy)- and 3,4,5-tris(decyloxy)-

Chart 1

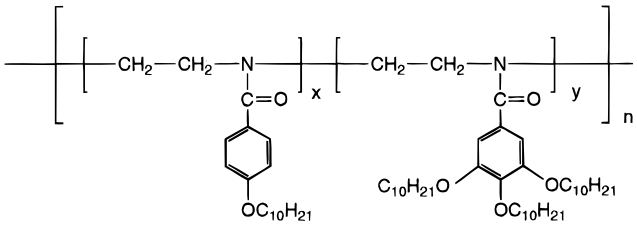

LPEI(22)-Co4/3,4,5

benzoyl side groups in a 1:1 ratio (Chart 1). **LPEI(22)-3,5** only exhibits a glass transition to the isotropic state at 40 °C. The statistical copolymer **LPEI(22)-Co4/3,4,5** shows homogeneous birefringence under the polarizing microscope above the glass transition ($T_g \approx 56$ °C) up to 90 °C, but this is probably not related to a hexagonal columnar mesophase. Reserving further investigations, we attribute this behavior to a partial crystallinity of the polymer. It should be noted in this context that a 1:1 mixture of the homopolymers **LPEI(22)-4** and **LPEI(22)-3,4,5** is not a homogeneous material. The two polymers do not mix and show their individual phase transitions. An equivalent copolymer bearing a 2:1 excess of the 3,4,5-tris(decyloxy)benzoyl side group only shows a glass transition to the isotropic state at 55 °C. In similarity to the behavior of the macrocyclic model compounds, these observations again emphasize the unique feature of the 3,4-bis(decyloxy)benzoyl side group with regard to the formation of hexagonal columnar mesophases.

In addition, the importance of the side-chain packing in the mesophase formation is expressed by the lower clearing temperature of the 3,4-bis(heptyloxy)benzoyl-substituted **LPEI(22)-3,4/7**, in which the alkyl groups are shorter by three methylene groups. The clearing temperature is lowered by 17 °C, and the clearing point can be supercooled by 19 °C (in the case of the series **LPEI(*n*)-3,4** with pendant decyloxy chains, supercooling amounts only to 10−13 °C, depending on the molecular weight). In addition, due to the kinetic hindrance of the mesophase formation for the shorter side-chain length, an isotropic glass is obtained by supercooling the material from the isotropic state. In the DSC heating curve (not shown) of such an isotropic glass, a strong endothermic peak at 71 °C above the glass transition is detected which can be related to a re-entry into the liquid crystalline phase of the material on heating, in accordance with polarizing microscopy observations, whereas **LPEI(*n*)-3,4**-samples prepared under the same conditions appear birefringent under the polarizing microscope and do not show an endothermic peak in the DSC. The X-ray diffraction pattern of **LPEI(22)-3,4/7** in the mesophase does not show any higher-order reflections which are possibly too weak to be detected during our measurements. Although only an unspecific texture is observed under the polarizing microscope, we also assume a hexagonal columnar structure (ϕ_h) for this polymer.

Cinnamoyl-Substituted Oligo- and Polyamides. Motivated by the intriguing similarity of linear polyamides and cyclic oligoamides and in analogy to *N*-acylated azacrown derivatives,[38] we expected a liquid crystalline mesophase also for *N*-cinnamoyl-substituted poly(ethylenimine)s. As the *N*-benzoylated polymers, the compounds were obtained by polymer analogous conversion of linear poly(ethylenimine). According to

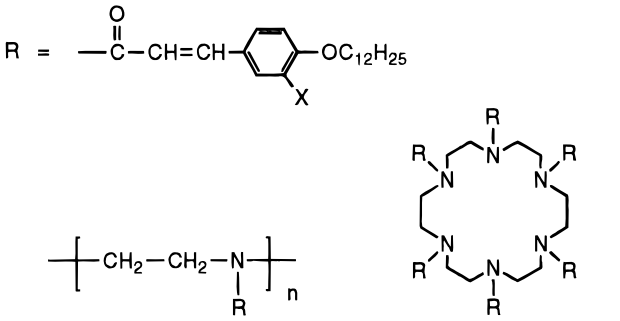

X = H	**LPEI(22)-Cinn12,H** c 180 (decomp)	**Cyc(6)-Cinn12,H** c 232 (D_x 209) i
X = OCH_3	**LPEI(22)-Cinn12,OMe** g 60 ϕ_h 251 i	**Cyc(6)-Cinn12,OMe** c 164 D_h 348 i

Figure 10. Phase behavior of *N*-cinnamoylated poly(ethylenimine)s and hexacyclenes: g, glassy; c, crystalline; D_h, discotic hexagonal mesophase; D_x, unspecified discotic mesophase; ϕ_h, hexagonal columnar mesophase; i, isotropic. Transition temperatures are given in °C.

^{1}H NMR spectroscopy and elemental analysis, the degree of substitution of both polymers consistently is above 95%.

The polymer **LPEI(22)-Cinn12,OMe** shows mesomorphic behavior under the polarizing microscope (g, 60 °C; lc, 251 °C i). On cooling from the isotropic state, a typical but unspecific texture is formed which does not change upon annealing the sample. Initially after cooling below the clearing point, biphasic regions are observed, and an additional texture is formed which disappears on further cooling. In the DSC curve, the clearing temperature observed on heating at 251 °C is supercooled by only 6 °C in the following cooling scan. In contrast to the observed biphasic behavior under the polarizing microscope, the peaks in the DSC measurements are rather sharp. However, a partial decomposition of the compound is reflected by a slightly decreased clearing temperature in the following DSC heating cycles, as well as by coloring of the substance under the polarizing microscope. In the X-ray flat camera picture of the substance (not shown here), three reflections in the ratio $1:3^{1/2}:2$ proving a hexagonal lattice are found. The (100) peak observed at 34.7 Å corresponds to a hexagonal lattice parameter of 40.1 Å.

In contrast, **LPEI(22)-Cinn12,H** does not melt without decomposition. On heating under the polarizing microscope, the color of the compound darkens significantly above 180 °C. In this case, the symmetry of the 4-substituted side group again results in a highly crystalline polymer with a melting point above the decomposition temperature. This observation is consistent with the behavior of hexacyclene derivatives bearing the same substituents (Figure 10). Note that the hexakis[4-(tetradecyloxy)cinnamoyl]hexacyclene with six C_{14} side chains exhibits a narrow hexagonal mesophase.[38,47]

The comparison with *N*-benzoylated polymers shows that the formation of a hexagonal columnar mesophase does not necessarily require two long alkyl chains as 3,4-substituents on the aromatic core. The described *N*-cinnamoylated polymers indeed confirm the necessity of a nonsymmetrical 3,4-substitution of the aromatic core, but the sterically less demanding methoxy group in 3-position next to the dodecyloxy chain serves sufficiently for the formation of a liquid crystalline phase.

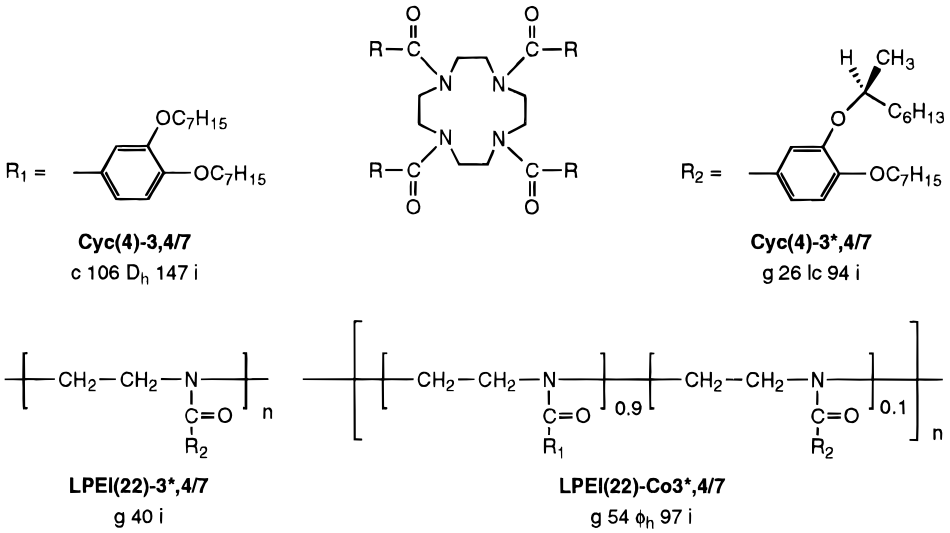

Figure 11. Phase behavior of oligo- and polyamides with chiral side groups: g, glassy; c, crystalline; D_h, discotic hexagonal mesophase; ϕ_h, hexagonal columnar mesophase; i, isotropic. Transition temperatures are given in °C.

Introduction of Chiral Groups. Due to the lack of a chiral center, the mesomorphic polymers **LPEI(*n*)-3,4** should form the same amounts of enantiomeric left- and right-handed helices. By introducing a chiral center either in the main chain or in the side chain, one of the two resulting diastereomeric conformers should be formed predominantly, and the chiral superstructure could then be identified by its chirooptical properties. Temperature-dependent ORD and CD spectra would give additional information about the polymer structure in the liquid crystalline state. In particular, it might be possible to detect whether a drastic change of the main-chain conformation such as a helix−coil transition occurs at the clearing point, or if simply the intercolumnar correlation is lost.

The comparison of two macrocyclic model compounds containing heptyloxy side groups, the achiral **Cyc(4)-3,4/7** and **Cyc(4)-3*,4/7**, which contains one (*S*)-(1-methylheptyl)oxy group in the 3-position, reveals that the introduction of a methyl group in α-position to the benzoyl unit extremely disturbs the columnar packing of the molecules and thus also the formation of a discotic mesophase (Figure 11). This is indicated by a lowering of the clearing point by about 50 °C. However, the crystallization of the material is suppressed as well, so that a liquid crystalline phase is still formed at lower temperatures.

For the analogous chiral linear polyamide **LPEI(22)-3*,4/7**, the clearing temperature may be shifted by approximately the same amount below the glass transition of the material at 40 °C, which in this case results in a complete loss of the mesomorphic properties. To reduce the undesired mesophase destabilization by the introduction of the branched side chains, a statistical copolymer containing only 10% of the chiral benzoyl groups has been synthesized. The behavior of this copolymer, **LPEI(22)-Co3*,4/7** (Figure 11), is very similar to that of the homopolymer **LPEI(22)-3,4/7** (Figure 9). An enantiotropic mesophase is formed, but with an observed supercooling of the isotropic state by 21 °C. In addition, the clearing temperature is lowered by 6 °C due to the presence of the chiral groups. The microscopic texture is rather unspecific, but in this case the hexagonal columnar structure of the mesophase could be proven by X-ray diffraction. The distances corresponding to the detected (100), (110), and (200) reflections were found to be in the characteristic ratio of $1:1/3^{1/2}:1/2$.

Chart 2

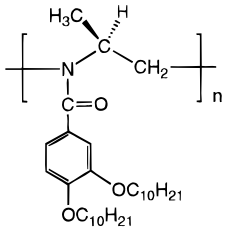

In contrast to the observed destabilization of the columnar packing by the introduction of chiral side groups, the synthesis of a linear poly(ethylenimine) with a chiral center in the main chain on first sight seems more promising. Based on molecular model calculations, a helical main-chain conformation has been already proposed for *N*-acylated poly(1-methylethylenimine).[48] The suggested 14_3-helix is in agreement with the structural parameters obtained from X-ray investigations on **LPEI(22)-3,4**. However, even in this case, the introduction of an additional methyl group disturbs the formation of an ordered columnar structure.

After the compound was initially obtained as a crystalline material melting at 63 °C, in the first cooling and second heating DSC scans of **ChPEI(30)-3,4** (Chart 2), only a glass transition at $T_g \approx 51$ °C is detected. Above the melting temperature, under the polarizing microscope, a nematic texture can be induced by shearing which disappears initially after the mechanical stress is released. This effect can be observed up to ∼90 °C, whereas in the DSC measurements no transition can be found at this temperature. In summary, a significant destabilization of the hexagonal columnar mesophase structure resulted from the introduction of chiral groups both into the side groups and into the polymer main chain. For the case of a chiral polymer backbone, this was rather surprising, since, based on the literature-described *N*-acylated poly(1-methylethylenimine),[48] the chiral center was assumed to advance a helical main-chain configuration. This may be seen as a support for the structural model discussed in Figure 7B, assuming a packing of several polymer chains into a single column. On the other hand, the additional methyl group in the ethyleneamine fragment may drastically

Scheme 2

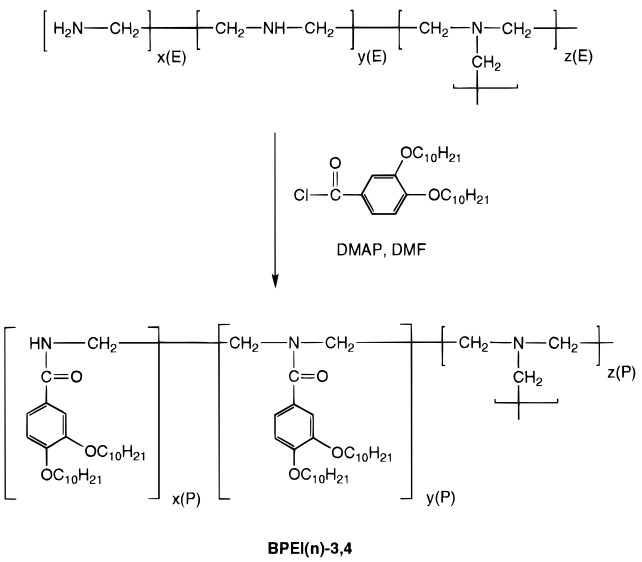

BPEI(n)-3,4

influence the orientation of the benzoyl side groups relative to the polymer main chain by changing the dihedral angle of the aryl−carbamide bond, thus explaining the distortion of the columnar structure in the single-chain model proposed in Figure 7A.

Statistically Branched *N*-Acylated Poly(ethylenimine)s. Commercially available, statistically branched poly(ethylenimine)s synthesized by cationic ring-opening polymerization of aziridines normally show a rather broad molecular weight distribution with primary, secondary, and tertiary amino units present in a ratio of 1:2:1, respectively. However, in oligomeric branched poly(ethylenimine)s used for the preparation of the *N*-acylated **BPEI(10)-3,4** and **BPEI(20)-3,4** (Scheme 2), the ratio between primary and tertiary amino units differs from 1:1 due to the use of diamines as termination reagents in the cationic polymerization of ethylenimine (see Table 3).[50−52] It has been shown that there is one short side branch per approximately 3.5 repeat units along the linear poly(ethylenimine) main chain.[52,61]

The polymer analogous acylation of the branched polymers was achieved, in analogy to the linear poly(ethylenimine)s, by reaction with 3,4-bis(decyloxy)benzoyl chloride using DMAP as a base.

However, in the case of the linear poly(ethylenimine)s **LPEI(*n*)-3,4**, a complete acylation of the amino units in the polymer backbone independent from the degree of polymerization was achieved, whereas the reaction of the branched samples is limited to the primary and secondary amino groups. In addition, these may not all be accessible during the reaction. In the ^{1}H NMR spectrum, tertiary as well as nonreacted primary and secondary amino groups are detected via the broad peak of the neighboring methylene protons at 2.6 ppm. According to the NMR data, it can be assumed that practically all primary and secondary amine units were acylated in the low molecular weight polymers **BPEI-(10)-3,4** and **BPEI(20)-3,4**. The calculated amount of methylene protons neighboring nonreacted amino groups correlates with the known content of tertiary amino groups in the corresponding branched starting polymers (Table 3), whereas in **BPEI(230)-3,4**, approximately 25% of the primary and secondary amino groups remain unconverted. These results are supported by elemental analysis.

In contrast to the linear polyamides, which form hexagonal columnar mesophases independent of the degree of polymerization, the phase behavior of the branched polymers is highly dependent on the molecular weight. The DSC curves of the three investigated samples **BPEI(*n*)-3,4** (n = 10, 20, 230) are shown in Figure 12A. The lowest molecular weight compound, **BPEI(10)-3,4**, exhibits a glass transition at 49 °C and a first-order transition at 115 °C, which in the cooling scan is detected at 106 °C. The clearing enthalpy of ΔH = 1.4 J g^{-1} is considerably lower than for the linear polymers, **LPEI(*n*)-3,4** (ΔH = 2.5 J g^{-1}). Under the polarizing microscope, the first-order transition in the DSC curve can be related to the isotropization of a fluid, birefringent phase. After the sample is cooled from the isotropic state into the mesophase, again a typical *focal conic* texture is formed (Figure 12B).

BPEI(20)-3,4 still shows a first-order transition at 111 °C, but the clearing enthalpy is only 0.4 J g^{-1}. In addition, a weak exothermic process is seen before the isotropization peak in the DSC. In the cooling curve (not shown here), only a glass transition related to the freezing of the isotropic melt can be observed. This is supported by the observations under the polarizing microscope. A sample quickly cooled from the isotropic state shows only a very weak birefringence, becoming more distinct after annealing the sample at 95 °C for 15 min. Thus, the formation of the liquid crystalline phase is kinetically controlled and can be suppressed by quickly supercooling the isotropic melt to room temperature. However, due to the low clearing enthalpy, a possible phase separation of amorphous and liquid crystalline regions has to be considered. In the same context, one may assume a lower order in the mesophase of the branched polyamide **BPEI(20)-3,4** as compared to the lower molecular weight sample **BPEI-(10)-3,4**. The highest molecular weight polymer synthesized in our work, **BPEI(230)-3,4**, shows no thermotropic liquid crystalline features at all. Even after annealing the sample above the glass transition of the material at 37 °C (see DSC heating scan in Figure 12A), no birefringence is observed under the polarizing microscope. Without further X-ray investigations, at this time the two weak peaks in the DSC heating scan cannot be clearly identified.

With increasing degree of polymerization, the described branched polyamides **BPEI(*n*)-3,4** lose the ability to form a thermotropic mesophase. Whereas the existence of a liquid crystalline state for the oligomeric **BPEI(10)-3,4** was clearly shown by DSC and polarizing microscopy, the high molecular weight polymer **BPEI-(230)-3,4** is an amorphous glass melting little above room temperature. Considering the phase behavior of the branched polyamides, the heterogeneity of the starting materials has to be taken into account as well. In the case of **BPEI(20)-3,4**, a lower molecular weight or less branched fraction may form a mesophase, which leads to a phase separation between liquid crystalline and isotropic parts of the sample.

The flat camera photograph taken from a fiber of **BPEI(10)-3,4** stretched in the mesophase is shown in Figure 13. In the small-angle region, three reflections with a ratio of the corresponding layer distances of 1:1/$3^{1/2}$:1/2 are observed, which thus can be identified as (100), (110), and (200) reflections of a hexagonal packing with a lattice parameter a_{hex} larger by ∼2 Å than that found for the linear polyamides.

Table 3

	M_n[a]	M_w[a]	$x(E)$ (%)	$y(E)$ (%)	$z(E)$ (%)	$z(P)$ (%)	phase behavior
BPEI(10)−3,4	2900	3800	44	38	18	16	g, 49; ϕ_h, 115 i
BPEI(20)−3,4	4200	6600	40	35	25	23	g, 54; 1c, 111 i
BPEI(230)−3,4	60900	127900	25	50	25[b]	*c*	g, 37 i

[a] Obtained from GPC elugram ($CHCl_3$; standard, polystyrene). [b] References 50−52. [c] A calculation of this ratio from ^1H NMR data of the *N*-acylated polymer is not possible due to considerable broadening of the peaks.

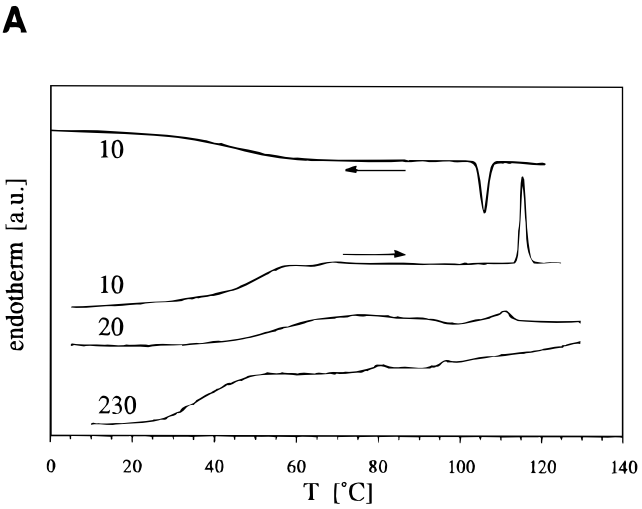

Figure 12. (A) DSC heating curves of the branched polyamides **BPEI(*n*)-3,4**; $n = 10$, 20, 230. The second heating scan is shown in all cases, as well as the first cooling curve obtained for **BPEI(10)-3,4** (scan rate, 10 °C min^{-1}). (B) Texture of **BPEI(10)-3,4** obtained after cooling from the isotropic state by 3 °C min^{-1} at 109 °C.

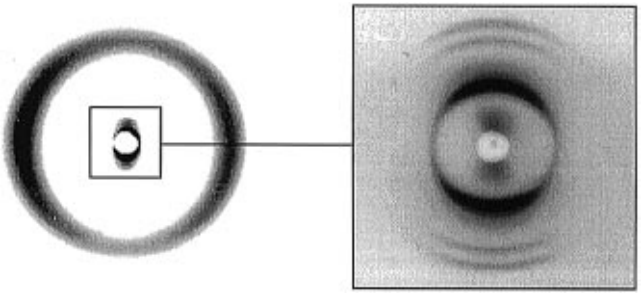

Figure 13. Flat camera photograph of an oriented sample of **BPEI(10)-3,4** obtained from a fiber stretched in the mesophase.

At first sight, the formation of a hexagonal columnar phase by the branched poly(ethylenimine) derivative **BPEI(10)-3,4** may contradict the previous assumption of a helically folded main-chain conformation in the linear polymers. Due to the low molecular weight of **BPEI(10)-3,4**, however, the polymer main chain bears only a low number of short side branches (mostly only one ethylene unit long) and still primarily consists of secondary amide units. Thus, only a slight deviation from the structure assumed for the linear polyamides has to be considered leading to a higher column diameter, which is, indeed, experimentally observed. Again, for the proof of the identity of the two mesophase structures, we investigated the thermal behavior of a mixture of the branched **BPEI(10)-3,4**, and linear **LPEI(22)-3,4** and we found miscibility of the two phases combined with the existence of a liquid crystalline mesophase (*fan-shaped* textures observed under the polarizing microscope) over the whole concentration range. The thermal phase behavior of a 1:1 mixture was determined from its DSC thermogram as g, 55 °C; ϕ_h, 114 °C i.

Interestingly, the branched **BPEI(10)-3,4** exhibits an even broader mesophase range with a clearing temperature 16 °C higher than that of the linear **LPEI(11)-3,4**, which has approximately the same molecular weight. Thus, the presumably imperfect helical order of the linear polymer main chain not only tolerates the introduction of a few distortions without losing the material's mesomorphic features but seems to be even stabilized by a low number of short side branches. However, the increasing length of the side chains as well as the higher number of branches in the higher molecular weight polymers completely suppresses the formation of a thermotropic liquid crystalline state.

Regularly Branched *N*-Acylated Oligoamines. In contrast to the statistically branched poly(ethylenimine)s described in the previous paragraph, dendrimeric oligo- and polyamines consist of a "self-resembling" branched structure with tertiary amino groups in the inner region and primary amino units at the periphery of the spherical molecule. The ratio between primary and tertiary units is given by the "generation number", and, in an ideal moleule, no secondary amino units should exist.[62−64] In our work, a branched oligoamine—which may be viewed as a first generation dendrimer—was acylated with benzoyl side groups bearing different numbers of decyloxy substituents. The phase behavior of the three *N*-acylated regularly branched oligoamines **BN(6)-4**, **BN(6)-3,4** and **BN(6)-3,4,5**, with one, two and three alkyl groups per benzamide unit, respectively, is shown in Figure 14. It should be noted, however, that comparison of these compounds with statistically branched poly(ethylenimine) derivatives is limited due to the presence of the propylene units.[64]

As in the case of the linear poly(ethylenimine) derivatives, only **BN(6)-3,4**, with the 3,4-bis(decyloxy) unit, shows liquid crystalline properties; the two other samples exhibit only crystalline phases. The DSC thermogram of **BN(6)-3,4** shows the monotropic nature of the mesophase. Nevertheless, the transition from the isotropic to the liquid crystalline phase, observed at 88 °C on cooling, can be found in the heating scan as well, as long as the sample is not cooled below 60 °C or annealed in the metastable phase.

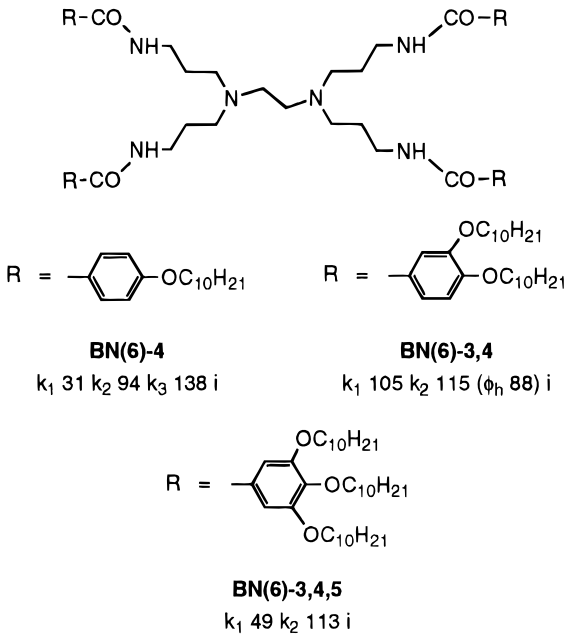

Figure 14. Phase behavior of regularly branched *N*-acylated oligoamines **BN(6)-4**, **BN(6)-3,4** and **BN(6)-3,4,5**: k, crystalline; ϕ_h, hexagonal columnar mesophase; i, isotropic. Phase transition temperatures are given in °C. For an analytically pure sample of **BN(6)-4** next to the transition at 138 °C (ΔH = 99.1 kJ mol^{-1}), an additional peak is observed at 149 °C (ΔH = 3.0 kJ mol^{-1}). Under the polarizing microscope, the melting of the majority of the crystals can be seen at 138 °C; above that temperature, small domains of the sample still exist in a different crystal modification surrounded by an isotropic matrix. These small domains melt at 149 °C.

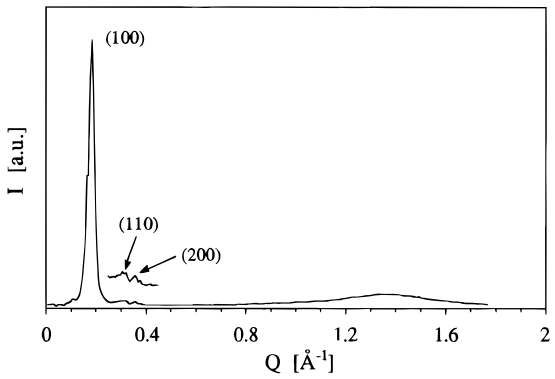

Figure 15. X-ray diffraction pattern of **BN(6)-3,4** in the monotropic mesophase (obtained from the flat camera picture by integration over the entire detector range).

In principle, both smectic and discotic structures may be considered for the mesophase of **BN(6)-3,4**, depending on the molecular conformation being either stretched or disklike in the mesophase. In the X-ray diffraction pattern of the monotropic mesophase (Figure 15), three reflections are seen, which again—as for the other hexagonal mesophases described in this paper—give the characteristic ratio of 1:1/3$^{1/2}$:1/2 for the corresponding layer distances.

Thus, a hexagonal columnar mesophase is also formed by **BN(6)-3,4**, which again is supported by the observation of a spherolitic structure with homeotropically oriented regions under the polarizing microscope. Concerning the molecular structure, a disklike conformation is possible; due to the relatively large free volume in the center region of the molecules, however, it seems rather unlikely that only one single molecule forms the constituting unit of the columnar mesophase. Possibly, as in the case of a series of metallomesogens described by Swager *et al.*,[65−68] a "time-averaged" dimerization of two molecules may be assumed. In addition, based on the model for the columnar packing of ethylene bisamides proposed by Percec *et al.*,[19] one may speculate about the possible formation of semi-columns induced by hydrogen bonds between the secondary amide units. In this context, a more detailed insight into the aggregation of the molecules into a columnar structure could be gained from measurements of the density combined with an accurate measurement of the intercolumnar distance, which is complicated by the metastability of the mesophase.

Whereas for **BN(6)-4** a smectoid geometry of the molecules is suggested, **BN(6)-3,4,5** should rather adopt a disklike conformation. Only **BN(6)-3,4**, with an intermediate side-chain density, forms a liquid crystalline mesophase, which—also for these regularly branched systems—points to the very special mesogenic feature of the 3,4-bis(decyloxy)benzoylamide unit.

The central ethyleneamine unit of these branched compounds should easily give access to a tailoring of the liquid crystalline properties by complexation of transition metal ions,[69] as the tendency toward the formation of microphase separated structures would be enhanced and, moreover, the conformational flexibility of the molecules would be reduced. In a similar fashion, the hydrochlorides of these compounds should be able to form mesomorpic phases.[70] This was shown recently for a similar branched oligomer.[71] Higher generation dendrimers were not investigated so far, but since these molecules tend to adopt a spherical structure with the reactive units on the surface, we do not expect mesomorphic materials for the higher generations of regularly branched *N*-acylated polyamines.

Conclusions

The observation of mesomorphic properties for the materials described in this paper shows the extraordinary power of the *N*-[3,4-bis(decyloxy)benzoyl]ethyleneamine fragment toward the induction of hexagonal columnar mesophases in oligo- and polyamides of different molecular architecture, although the "monomer" 3,4-bis(decyloxy)benzoyl-*N*,*N*-dimethylamide is not liquid crystalline. Only the special packing behavior in oligomeric as well as polymeric systems leads to the observed mesophases. Based on the well-investigated phase behavior of macrocyclic oligoamides, the manifold possibilities for the variation of structural parameters might lead to a great number of new mesomorphic materials. Many structural principles known from the mesophase formation in macrocyclic materials could be transferred into the area of linear polymers. Finally, as the constituting unit, the *N*-acylated ethyleneamine fragment, is identical in the linear polymers and the cyclic low molecular weight compounds, the described systems bridge the gap between thermotropic discotic mesophases and liquid crystalline columnar structures formed by linear polymers.

Acknowledgment. The authors thank Dr. Wolfgang Paulus (BASF AG, Ludwigshafen, Germany) for providing the branched and dendrimeric oligomers and Dr. Dieter Schollmeyer (Institut für Organische Chemie, Universität Mainz, Germany) for the X-ray structural analysis of ethyl 4-(heptyloxy)-3-hydroxybenzoate.

Supporting Information Available: Characterization data for ethyl 4-(heptyloxy)-3-hydroxybenzoate, ethyl 4-(hep-

tyloxy)-3-[(*S*)-(1-methylheptyl)oxy]benzoate, **N(5)-3,4**, **LPEI-(22)-4**, **LPEI(22)-3,4,5**, **LPEI(22)-3,5**, **LPEI(22)-Cinn12,H**, **LPEI(22)-Cinn12,OMe**, **LPEI(22)-3,4/7**, and **LPEI(22)-3*,4/7** (3 pages). Ordering information is given on any current masthead page.

References and Notes

(1) de Gennes, P. G. *The physics of liquid crystals*; Clarendon Press: Oxford, 1974.
(2) Vertogen, G.; de Jeu, W. H. *Thermotropic Liquid Crystals, Fundamentals*; Springer-Verlag: Berlin, 1988.
(3) Ungar, G. *Polymer* **1993**, *34*, 2050−2059.
(4) Chandrasekhar, S.; Sadashiva, B. K.; Suresh, K. A. *Pramana* **1977**, *9*, 471.
(5) Levelut, A. M. *J. Chim. Phys.* **1983**, *80*, 149.
(6) Chandrasekhar, S. *Liq. Cryst.* **1993**, *14*, 3.
(7) Bauer, S.; Plesnivy, T.; Ringsdorf, H.; Schuhmacher, P. *Makromol. Chem., Macromol. Symp.* **1992**, *64*, 19−32.
(8) Brienne, M.-J.; Gabard, J.; Lehn, J.-M.; Stibor, I. *J. Chem. Soc., Chem. Commun.* **1989**, 1868.
(9) Lehn, J.-M. *Makromol. Chem., Macromol. Symp.* **1993**, *69*, 1−17.
(10) Bunning, J. D.; Lydon, J. E.; Eaborn, C.; Jackson, P. M.; Goodby, J. W.; Gray, G. W. *J. Chem. Soc., Faraday Trans. 1* **1982**, *78*, 713.
(11) Lattermann, G.; Staufer, G. *Liq. Cryst.* **1989**, *4*, 347.
(12) Eckert, A.; Kohne, B.; Praefcke, K. *Z. Naturforsch. B* **1988**, *43*, 878.
(13) Praefcke, K.; Levelut, A. M.; Kohne, B.; Eckert, A. *Liq. Cryst.* **1989**, *6*, 263.
(14) Jeffrey, G. A.; Wingert, L. M. *Liq. Cryst.* **1992**, *12*, 179.
(15) Spegt, P. A.; Skoulios, A. E. *Acta Crystallogr.* **1966**, *21*, 892.
(16) Malthête, J.; Levelut, A. M. *Adv. Mater.* **1991**, *3*, 1991.
(17) Malthête, J.; Collet, A. *J. Am. Chem. Soc.* **1987**, *109*, 7544−7545.
(18) Malthête, J.; Collet, A.; Levelut, A. M. *Liq. Cryst.* **1989**, *5*, 123−131.
(19) Percec, V.; Heck, J.; Johansson, G.; Tomazos, D.; Kawasumi, M.; Ungar, G. *J. Macromol. Sci.−Pure Appl. Chem.* **1994**, *A31*, 1031−1070.
(20) Percec, V.; Heck, J.; Johansson, G.; Ungar, G. *Polym. Prepr.* **1993**, *34*, 116−117.
(21) Percec, V.; Lee, M.; Heck, J.; Blackwell, H. E.; Ungar, G.; Alvarez-Castillo, A. *J. Mater. Chem.* **1992**, *2*, 931−938.
(22) Kwon, Y. K.; Chvalun, S.; Schneider, A. I.; Blackwell, J.; Percec, V.; Heck, J. A. *Macromolecules* **1994**, *27*, 6129−6132.
(23) Percec, V.; Heck, J.; Tomazos, D.; Falkenberg, F.; Blackwell, H.; Ungar, G. *J. Chem. Soc., Perkin Trans. 1* **1993**, 2799−2811.
(24) Kwon, Y. K.; Chvalun, S. N.; Blackwell, J.; Percec, V.; Heck, J. A. *Macromolecules* **1995**, *28*, 1552−1558.
(25) Johansson, G.; Percec, V.; Ungar, G.; Zhou, J. P. *Macromolecules* **1996**, *29*, 646−660.
(26) Percec, V.; Johansson, G.; Schlueter, D.; Ronda, J. C.; Ungar, G. *Macromol. Symp.* **1996**, *101*, 43−60 and references cited therein.
(27) Percec, V.; Schlueter, D.; Ronda, J. C.; Johansson, G.; Ungar, G.; Zhou, J. P. *Macromolecules* **1996**, *29*, 1464−1472.
(28) Watanabe, J.; Takashina, Y. *Macromolecules* **1991**, *24*, 3423−3426.
(29) Weber, P.; Guillon, D.; Skoulios, A. *Liq. Cryst.* **1990**, *8*, 825−837.
(30) Frey, H.; Matyjaszewski, K.; Möller, M.; Oelfin, D. *Colloid Polym. Sci.* **1991**, *269*, 442.
(31) Yamagishi, T.; Fukuda, T.; Miyamoto, T.; Yakoh, Y.; Takashina, Y.; Watanabe, J. *Liq. Cryst.* **1991**, *10*, 467−473.
(32) Kojima, M.; Magill, J. H. *Polymer* **1989**, *30*, 579.
(33) Ungar, G.; Feijoo, J. L.; Percec, V.; Yourd, R. *Macromolecules* **1991**, *24*, 953−957.
(34) Isoda, S.; Kawaguchi, A.; Katayama, K. I. *J. Polym. Sci., Polym. Phys. Ed.* **1984**, *22*, 669.
(35) Lehn, J. M.; Malthête, J.; Levelut, A. M. *J. Chem. Soc., Chem. Commun.* **1985**, 1794−1795.
(36) Idziak, S. H. J.; Maliszewskyj, N. C.; Heiney, P. A.; McCauley, J. P., Jr.; Sprengeler, P. A.; Smith, A. B., III. *J. Am. Chem. Soc.* **1991**, *113*, 7666−7672.
(37) In contrast to this, Zhang and Moore described discogens based on macrocyclic phenylacetylene derivatives which, due to their stiffness, indeed posses a central hole with a diameter of approximately 8 Å: Zhang, J.; Moore, J. S. *J. Am. Chem. Soc.* **1994**, *116*, 2655−2656.
(38) Mertesdorf, C.; Ringsdorf, H. *Liq. Cryst.* **1989**, *5*, 1757−1772.
(39) Lattermann, G. *Liq. Cryst.* **1989**, *6*, 619.
(40) Fischer, H.; Ghosh, S. S.; Heiney, P. A.; Maliszewskyj, N. C.; Plesnivy, T.; Ringsdorf, H.; Seitz, M. *Angew. Chem., Int. Ed. Engl.* **1995**, *34*, 795−797.
(41) Stebani, U.; Lattermann, G. *Macromol. Rep.* **1995**, *A32*, 385−401.
(42) Stebani, U.; Lattermann, G.; Wittenberg, M.; Festag, R.; Wendorff, J. H. *Adv. Mater.* **1994**, *6*, 572−574.
(43) Stebani, U.; Lattermann, G.; Festag, R.; Wittenberg, M.; Wendorff, J. H. *J. Mater. Chem.* **1995**, *5*, 2247−2251.
(44) Han, M. J.; Chang, J. Y.; Lee, Y. Y. *Macromolecules* **1982**, *15*, 255−258.
(45) Kobayashi, S.; Saegusa, T. In *Ring Opening Polymerization*; Ivin, K. J., Saegusa, T., Eds.; Elsevier Applied Science Publishers: Essex, 1984; Vol. 2, pp 761−807.
(46) Kobayashi, S. *Prog. Polym. Sci.* **1990**, *15*, 751.
(47) Mertesdorf, C.; Ringsdorf, H. *Mol. Eng.* **1992**, *2*, 189−212.
(48) Oh, Y. S.; Yamazaki, T.; Goodman, M. *Macromolecules* **1992**, *25*, 6322−6331.
(49) Witte, H.; Seeliger, W. *Liebigs Ann. Chem.* **1974**, 996.
(50) Jones, G. D.; Mac Williams, D. C.; Braxtor, N. A. *J. Org. Chem.* **1965**, *30*, 1994.
(51) Johnson, T. W.; Klotz, I. *Macromolecules* **1974**, *7*, 149−153.
(52) Dick, C. R.; Ham, G. E. *J. Macromol. Sci., Chem.* **1970**, *4*, 1301.
(53) Fontes, E.; Heiney, P.; Ohba, M.; Haseltine, J. M.; Smith, A. B., III. *Phys. Rev. A* **1988**, *37*, 1329.
(54) Chiang, L. Y.; Safinya, C. R.; Clark, N. A.; Liang, K. S.; Bloch, A. N. *J. Chem. Soc., Chem. Commun.* **1985**, 695.
(55) Schaub, M.; Mathauer, K.; Schwiegk, S.; Albouy, P.-A.; Wenz, G.; Wegner, G. *Thin Solid Films* **1992**, *210/211*, 397−400.
(56) Litt, M.; Rahl, F.; Roldan, L. G. *J. Polym. Sci., A-2* **1969**, *7*, 463−473.
(57) Rodriguez-Parada, J. M.; Percec, V. *J. Polym. Sci. A, Polym. Chem.* **1987**, *25*, 2269−2279.
(58) Chatani, Y.; Tadokoro, H.; Saegusa, T.; Ikeda, H. *Macromolecules* **1981**, *14*, 315−321.
(59) Chatani, Y.; Kobatake, T.; Tadokoro, H.; Tanaka, R. *Macromolecules* **1982**, *15*, 170−176.
(60) Liebmann, A.; Mertesdorf, C.; Plesnivy, T.; Ringsdorf, H.; Wendorff, J. H. *Angew. Chem., Int. Ed. Engl.* **1991**, *30*, 1375−1377.
(61) Lukovkin, G. M.; Pshezhetsky, V. S.; Murtazaeva, G. A. *Eur. Polym. J.* **1973**, *9*, 559.
(62) Tomalia, D. A.; Killat, G. R. In *Encyclopedia of Polymer Science and Engineering*, 2nd ed.; Mark, H. F., Bikales, N. M., Overberger, C. G., Menges, G., Kroschwitz, J. I., Eds.; Wiley & Sons: New York, 1985; Vol. 1, pp 680−739.
(63) Tomalia, D. A. *Adv. Mater.* **1994**, *6*, 529.
(64) Dendrimeric poly(ethylenimine)s were described by Tomalia: Tomalia *et al.*: D. A.; Naylor, A. M.; Goddard, W. A., III. *Angew. Chem.* **1990**, *102*, 1990.
(65) Lai, C. K.; Serrette, A. G.; Swager, T. M. *J. Am. Chem. Soc.* **1992**, *114*, 7948.
(66) Serrette, A. G.; Swager, T. M. *J. Am. Chem. Soc.* **1993**, *115*, 8879.
(67) Zheng, H.; Lai, C. K.; Swager, T. M. *Chem. Mater.* **1994**, *6*, 101.
(68) Serrette, A. G.; Lai, C. K.; Swager, T. M. *Chem. Mater.* **1994**, *6*, 2252.
(69) Fischer, H.; Plesnivy, T.; Ringsdorf, H.; Seitz, M. *J. Chem. Soc., Chem. Commun.* **1995**, 1615−1616.
(70) Lattermann, G.; Schmidt, S.; Gallot, B. *J. Chem. Soc., Chem. Commun.* **1992**, 1091−1092.
(71) Stebani, U.; Lattermann, G. *Adv. Mater.* **1995**, *7*, 578−581.

MA960270V